SUPERINTENDENCIA DE INDUSTRIA Y COMERCIO

RAD: 14-98853- -9 **FECHA**: 2015-09-10 07:30:16
DEP: 2020 DIRECCION DE NUEVAS CREACIONES **EVE:** 378 FASE NACIONAL INCLUIDO CAPITULO I
TRA: 11 PCT-PATENTE DE INVENCION CAPITULOS I Y II **FOLIOS**: 6
ACT: 519 TRASLADOINFORME

DIRECCIÓN DE NUEVAS CREACIONES

2020
Bogotá, D.C.,

Abogado(a)/Señor(a)
ANDREA TOBOS MATEUS

Asunto: Radicación: 14-98853- -9
Trámite: 11
Evento: 378
Actuación: 519
Oficio: 10622
Folios: 6

Patente de Invención	X			Patente de Modelo de Utilidad	
Vía Nacional					
Vía PCT (Fase Nacional)	X	Capítulo I	X	Capítulo II	
No. Solicitud Internacional	PCT/US2012/059708				
Fecha de Presentación Internacional	11/10/2012				

Como resultado del examen de fondo realizado, con fundamento en el Artículo 45 de la Decisión 486 de la Comisión de la Comunidad Andina, se comunica:

1. Documentos estudiados

Descripción:	Radicado N° 14-98853-00000-0000	08/Mayo/2014
Reivindicaciones:	Radicado N° 14-98853-00000-0000	08/Mayo/2014
	Radicado N° 14-98853-00001-0000	13/Mayo/2014
	Radicado N° 14-98853-00005-0000	28/Julio/2014
	Radicado N° 14-98853-00007-0000	23/Enero/2015
Dibujos:	Radicado N° 14-98853-00000-0000	08/Mayo/2014
Secuencias:	Radicado N° 14-98853-00000-0000	08/Mayo/2014
Prioridad:	US 61/546,248	12/Octubre/2011

2. Análisis de la Prioridad

Se acepta la reivindicación de prioridad porque ésta solicitud fue presentada dentro del plazo establecido (Art. 9 D 486) y su contenido técnico corresponde con el de la prioridad reivindicada.

3. Modificaciones aceptadas (Art 34 D 486 y Art 19, 22 y 34 PCT)

Se aceptan las modificaciones a las reivindicaciones en los folios 3 a 6 del Radicado N° 14-98853-00007-0000, ya que no amplían la materia inicialmente presentada, y sobre dicho capítulo se realiza el análisis de patentabilidad.

4. Objeto de la invención

De acuerdo con lo establecido en el numeral 1.2.2.2 del Título 10 de la Circular Única para efectos del examen de patentabilidad, se tendrá en cuenta la tasa pagada por el solicitante al momento de comenzar el examen para las reivindicaciones adicionales; esto es que cuando la solicitud contenga más de diez (10) reivindicaciones y no se haya pagado la tasa complementaria, sólo se estudiarán las cubiertas por la tasa pagada. En el presente caso se estudiarán las reivindicaciones 1 a 19 del capítulo reivindicatorio del Radicado N° 14-98853-00007-0000.

Título de la solicitud: “PROTEÍNA NAGLU HUMANA RECOMBINANTE Y USOS DE LA MISMA”

El problema planteado en esta solicitud consiste en la necesidad de proporcionar una proteína NaGlu estable que sea enzimáticamente activa y que tenga propiedades físicas que le permitan atravesar la barrera hematoencefálica (BHE) e introducirse de manera eficaz en los lisosomas de las células diana, para su uso terapéutico, por ejemplo, en el tratamiento del síndrome de Sanfilippo de tipo B.

Para resolver este problema técnico la solicitud en estudio proporciona composiciones que comprenden la proteína NaGlu humana recombinante (rhNaGlu).

El objeto de la presente solicitud se relaciona con la Clasificación Internacional de Patentes (CIP): A61K38/47; C12N5/07; C12N9/26.

5. Excepción a la Patentabilidad (Art 20 D 486 literal (d))

El objeto de las reivindicaciones 15 – 17 y 19 no es patentable de acuerdo con el art citado, debido a que definen una composición que comprende una mezcla aislada de N – acetil – α – D –glucosaminidasa (rhNaGlu), afirmando que dicha composición permite cruzar la barrera de sangre del cerebro de un mamífero que presenta deficiencia de NaGlu, cuando es administrada sistemáticamente de manera intravenosa, haciendo referencia a un método de tratamiento de una enfermedad. Se le recuerda a la solicitante que los métodos terapéuticos para el tratamiento humano o animal, así como los métodos de diagnóstico aplicados a los seres humanos o animales, no son patentables, de acuerdo al artículo citado.

6. De la solicitud de patente

Titulo

El título de la solicitud de la patente de invención contiene la palabra “*usos*” y de acuerdo con el Art. 14 D 486, los usos no son patentables, por lo cual se sugiere a la solicitante hacer la corrección necesaria.

Reivindicaciones (Art 30 D 486, Art 22 PCT)

1– Las reivindicaciones 1, 7 - 11 no son claras porque definen una composición que comprende una mezcla aislada de N – acetil – α – D – glucosaminidasa recombinante (rhNaGlu), en términos de su resultado alcanzar que da cuenta de su mecanismo de acción, al indicar que "*una o más estructuras de glucano que comprenden manosa – 6 – fosfato (M6P) para que dicho M6P que contiene rhNaGlu sea internalizado en una célula de mamífero que tiene deficiencia de NaGlu por endocitosis mediada por el receptor de M6P y restablece por lo menos 50% de la actividad de NaGlu observada en una célula del tipo natural del mismo tipo que expresa la NaGlu endógena; que dicha rhNaGlu restablece entre el 60, 70, 80, 90, 95 o 100% de la actividad enzimática normal de NaGlu*; *que dicha célula de mamífero deficiente en NaGlu es una célula humana"*, y que *"rhNaGlu es producida de una célula de oviducto de una ave transgénica"*. En este caso las reivindicaciones incluirían no sólo la solución propuesta por el solicitante, sino todas las alternativas presentes o futuras que lleguen a ese resultado. Se le recuerda a la solicitante que una composición farmacéutica se debe definir a partir de sus características técnicas esenciales, especificando sus ingredientes, excipientes en las cantidades o proporciones específicas características de dicha composición.

2– La reivindicación 4 no es clara por que menciona que la rhNaGlu comprende N – acetilflucosamina (GlcNAc), la cual hace referencia a una molécula de azúcar no existente. Se le sugiere a la solicitante corregir la redacción de la reivindicación mencionando el azúcar "*N – acetil glucosamina*" o "*N – acetil fucosamina*".

3– La reivindicación 10 no es clara porque hace referencia a la producción de rhNaGlu, y no se define dicho proceso a partir de una secuencia lógica de etapas que permitan llegar a la obtención de la proteína recombinante. Adicionalmente se menciona que rhNaGlu es producida de una célula de oviducto, de la cual no es claro si hace referencia a una célula transgénica. Se sugiere a la solicitante modificar la redacción de la reivindicación mencionada especificando la línea celular a ser transformada, su origen y tipo de célula.

4– Las reivindicaciones 1 y 11 no son claras porque definen una composición que comprende una mezcla aislada de N – acetil – α – D – glucosaminidasa (rhNaGlu), en términos de que esta contiene una o más estructuras de glucano, lo cual corresponde a una definición muy general de este tipo de carbohidratos, que dificulta entender el alcance de la reivindicación y su diferenciación con el estado de la técnica.

5– Las reivindicaciones 1 y 11, no son concisas porque reclaman de forma repetitiva una composición que comprende la proteína N – acetil – α – D – glucosaminidasa (rhNaGlu), en más de una reivindicación independiente. Se le recuerda a la solicitante que por categoría inventiva de producto solo puede haber una reivindicación independiente y las demás si son verdaderas modalidades deben presentarse en la forma de reivindicaciones dependientes.

6– Las reivindicaciones 2 – 6, 12 - 14 no son claras porque no definen el patrón de glicosilación específico o proporción molar, en el cual los monosacáridos manosa - 6-fosfato (M6P), N – acetilglucosamina (GlcNAc), galactosa y N – acetilgalactosamina (GalNAc) se adicionan a la proteína NaGlu, y cuál de estas moléculas es glicosilada enlazada a N u O. Se le recuerda a la solicitante que es indispensable definir el patrón de glicosilación, debido a su importancia en la respuesta del sistema inmune.

7– Las reivindicaciones 1, 2 11 y 14 no son claras porque los términos *"mezcla aislada",* "*cantidad suficiente*", "*una o más*", "*al menos*" y "*aproximadamente*" son imprecisos y no limitativos, por lo cual no permiten distinguir la invención del estado de la técnica. Se sugiere sustituirlo por un término o rango concreto.

Descripción (Art 28 D 486)

Debido a que la solicitud se refiere a una rhNaGlu obtenida a partir de un huevo de un ave transgénica que expresa dicha proteína en células del oviducto, que se secretan en el lumen y se depositan en la clara del huevo, es necesario presentar el Certificado de Depósito para la línea celular de células del oviducto.

7. Determinación del Estado de la Técnica

El estado de la técnica se determinó con base en la fecha de presentación de la solicitud de prioridad: 12 de octubre de 2011, y se encontraron los siguientes documentos que anticipan el objeto de esta solicitud:

Ítem	Documento	Título	Fecha de Publicación
D1	WO2009/131698	"Phosphorylated Recombinant N-Acetyl-alpha-D- Glucosaminidase (NaGlu) and uses thereof"	29/Octubre/2009
D2	Di Natale P *et al.*, 2005*. Biochem. J*. Vol. 388, Pág. 639 – 646.	"Treatment of the mouse model of mucopolysaccharidosis type IIIB with lentiviral-NAGLU vector"	13/Enero/2005
D3	Jung – Ja P. K. *et al.,* 2009*. Structural Biology.* Vol. 19, Pág. 534 – 542.	"Carbohydrate recognition by the mannose-6-phosphate receptors"	Octubre/2009

El documento D1[1] divulga proteínas de fusión recombinantes NaGl fosforiladas, métodos de producción y usos de las mismas (Abstract).

El documento D2[2] divulga un estudio en el que emplean un vector lentiviral que comprende ADNc de NAGLU humana, conducido por un citomegalovirus (CMV) como promotor para la transducción *in vivo* del gen terapéutico, en el modelo murino para el síndrome de Sanfilippo tipo B (MPS IIIB) por administración intravenosa (Pág. 639, Col. 2).

El documento D3[3] divulga avances en los análisis estructurales de los receptores de manosa – 6 – fosfato (M6P) catión – dependiente (CD – MPR) y de manosa – 6 – fosfato (M6P) catión – independiente (CI – MPR), que evidencian las bases estructurales para el reconocimiento de los residuos fosfomanosílicos, proporcionando una mayor comprensión acerca de cómo cargan y descargan su carga esta clase de receptores (Abstract).

8. Examen de Patentabilidad (Art 14 D486)

Novedad (Art 16 D486)

La reivindicación 1 consiste en *"Una composición que comprende una mezcla aislada de N – acetil – alfa – glucosaminidasa (rhNaGlu) humana recombinante cuya secuencia de aminoácidos se expone en 24 a 743 de SEQ ID NO: 1, en la que dicha mezcla comprende una cantidad suficiente de rhNaGlu que contiene una o más estructuras de glucano que comprenden manosa – 6 – fosfato (M6P) ….."*. (Radicado Nº 14-98853-00007-0000)

Comparación de las características técnicas esenciales, con las del estado de la técnica:

Características esenciales	D1
Composición que comprende una mezcla aislada de N – acetil – alfa – glucosaminidasa (rhNaGlu) humana recombinante	Composición que comprende una proteína de fusión aislada recombinante que contiene N – acetil – alfa – glucosaminidasa (rhNaGlu) (Pág. 21, Rv. 19).
Comprende la secuencia de aminoácidos se expone en 24 a 743 de SEQ ID NO: 1	Proteína NaGlu comprende la SEQ ID NO: 1 o una secuencia de aminoácidos que presenta al menos 80% de identidad con la secuencia SEQ ID NO: 1 (Pág. 20, Rv. 12 –

1 http://worldwide.espacenet.com/publicationDetails/biblio?CC=WO&NR=2009131698A2&KC=A2&FT=D
2 http://www.ncbi.nlm.nih.gov/pubmed/15649123
3 http://www.sciencedirect.com/science/article/pii/S0959440X09001328

	Fig. 3B).
Comprende manosa – 6 – fosfato (M6P)	Proteína de fusión fosforilada con manosa – 6 – fosfato (Pág. 21, Rv. 19).

Las características esenciales de la reivindicación 1 habían sido divulgadas previamente en el documento D1, en el cual se divulgan composiciones que comprenden una proteína de fusión recombinante aislada fosforilada con manosa – 6 – fosfato y N – acetil – alfa – glucosaminidasa (NaGlu) y un portador farmacéuticamente aceptable y/o un medio de cultivo (Pág. 4, párr. 3). Dicha composición permite la internalización de la proteína de fusión recombinante humana (prhNaGlu) mediante endocitosis en una célula humana, que presenta deficiencia en la actividad enzimática de NaGlu y el incremento en la concentración de glucosaminoglucanos (GAG) (Pág. 16, párr. 3), con el objetivo de tratar una enfermedad autosómica recesiva de almacenamiento
lisosomal (LSD), como el síndrome de Sanfilippo de tipo B.

La proteína de fusión recombinante humana (prhNaGlu) comprende la SEQ ID NO: 1 o una secuencia de aminoácidos que presenta al menos 80% de identidad con la secuencia SEQ ID NO: 1 (Pág. 20, Rv. 12 - Pág. 4/30, Fig. 3B).

En consecuencia, la reivindicación 1 no es nueva, según lo divulgado en los documento D1.

Las reivindicaciones 2, 7 – 11, 14 y 18 no mencionan características novedosas para la composición de la reivindicación 1, por lo cual se considera que tampoco son nuevas.

Nivel inventivo (Art18 D486)

La reivindicación 3 consiste en "*La composición de la reivindicación 1, en la que dicha rhNaGlu comprende manosa".* (Radicado N° 14-98853-00007-0000)

Comparación de las características técnicas esenciales, con las del estado de la técnica:

Características esenciales	D2	D3
Composición que comprende una mezcla aislada de N – acetil – alfa – glucosaminidasa (rhNaGlu) humana recombinante	Inyección intravenosa de vector lentiviral – NaGlu que expresa la proteína NAGLU recombinante (Pág. 640, Col. 1 – Pág. 641, Col. 2).	N – acetil – alfa – glucosaminidasa (Pág. 535, Fig. 1)
Comprende la secuencia de aminoácidos se expone en 24 a 743 de SEQ ID NO: 1	ADNc de NaGlu humana (Pág. 640, Col. 1)	No registra
Comprende manosa – 6 – fosfato (M6P)	No registra	Enzima lisosomal que adquiere una etiqueta Man – 6 – P (Pág. 535, Fig. 1)
Manosa	No registra	Residuos de manosa sobre N – oligosacáridos (Pág. 535, Fig. 1)

El documento D2 se considera el estado de la técnica cercano a la invención definida en la reivindicación 3 porque divulga un vector lentiviral – NAGLU con el cual se demostró el potencial terapéutico en el tratamiento del síndrome de Sanfilippo tipo B (MPS IIIB) (Pág. 642, Col. 2), motivando al desarrollo de terapias génicas intravenosas alternativas que comprendan promotores específicos de tejidos y/o la aplicación de técnicas capaces de superar la barrera sanguínea, que podrían resultar en terapias más eficaces contra este tipo de síndromes a largo plazo (Pág. 645, Col. 2).

En cuanto al documento D3, divulga análisis estructurales de los receptores de manosa – 6 – fosfato (M6P) catión – dependiente (CD – MPR) y de manosa – 6 – fosfato (M6P) catión – independiente (CI – MPR), que revelan su interacción con los residuos fosfomanosílicos (Pág. 535, Col. 2).

La diferencia entre la invención, definida en la reivindicación 3 y la composición que comprende la proteína N – acetil – alfa – glucosaminidasa humana recombinante (rhNaGlu) divulgada en el documento D2, consiste en que la proteína rhNaGlu comprende manosa y manosa – 6 – fosfato (MP6).

El efecto que logra el incluir una composición farmacéutica que comprenda una mezcla aislada de N – acetil – alfa – glucosaminidasa humana recombinante (rhNaGlu), monosa y manosa – 6 – fosfato (MP6), es la internalización de la proteína de fusión recombinante humana (prhNaGlu) mediante endocitosis en una célula humana, que presenta deficiencia en la actividad enzimática de NaGlu.

Por lo tanto, el problema técnico objetivo que pretende resolver esta invención se puede formular así: “Como proveer una composición que comprende la proteína N - acetil- alfa - glucosaminidasa humana recombinante (rhNaGlu) estable, que sea enzimáticamente activa y que tenga propiedades físicas que le permitan atravesar la barrera hematoencefálica (BHE), que pueda ser internalizada por endocitosis en una célula de mamífero que tiene deficiencia de NaGlu, para tratar el síndrome de Sanfilippo de tipo B”.

Sin embargo, el documento D3 divulga que la fosforilación de N –glucanos en proteínas lisosomales permite la internalización celular de dichas proteínas y su posterior transporte hacia los lisosomas mediado por la interacción del receptor de M6P; además afirma, que las enfermedades autosómicas recesivas como el síndrome Sanfilippo tipo B se originan por la deficiencia en la actividad de la GlcNAc – fosfotransferasa, la cual es la enzima encargada de generar la etiqueta de M6P (Pág. 534, Col. 2), por lo cual para una persona normalmente versada en la materia seria obvio que la fosforilación de los residuos de manosa de la proteína NaGlu, incrementaría la concentración de esta enzima lisosomal, permitiendo el desarrollo de potenciales terapias de reemplazo enzimático, y por lo tanto el objeto reclamado por la solicitante no presenta altura inventiva a la luz de las enseñanzas de los documentos D2 y D3.

En consecuencia, la persona del oficio normalmente versada en la materia, incluiría las enseñanzas acerca de la fosforilación de los residuos de manosa de la proteína NaGlu, para incrementar la concentración de esta enzima lisosomal divulgadas en el documento D3, en el procedimiento para la producción de vectores lentivirales que comprenden una la proteína N - acetil- alfa - glucosaminidasa humana recombinante (rhNaGlu) divulgado en el documento D2 para llegar así al objeto de la reivindicación 3 de la solicitud, por lo cual se considera obvia.

En conclusión, la reivindicación 3 cumple el requisito de novedad (Art. 16), pero no cumple con el requisito de nivel inventivo (Art. 18).

Las reivindicaciones dependientes 4 – 6, 12 - 13 no mencionan características inventivas adicionales para la composición de la reivindicación 3, por lo cual se considera que tampoco tienen nivel inventivo.

9. Conclusión

Los requisitos de Patentabilidad de la presente solicitud están afectados así:

Ítem	Documento	Reivindicaciones afectadas	Requisito que afecta
D1	WO2009/131698	2, 7 – 11, 14 y 18	Novedad
D2	Di Natale P *et al*., 2005. Biochem. J. Vol. 388, Pág. 639 – 646.	3 – 6, 12 – 13	Nivel inventivo
D3	Jung – Ja P. K. *et al.,* 2009. Structural Biology. Vol. 19, Pág. 534 – 542.	3 – 6, 12 – 13	Nivel inventivo

En cumplimiento del artículo 45 de la Decisión 486 de la Comisión de la Comunidad Andina, se le indica que debe dar respuesta dentro del término de sesenta (60) días contados a partir del día siguiente de la fecha de notificación de la presente comunicación. En caso de no dar respuesta al presente requerimiento, o si a pesar de la respuesta subsistieran los impedimentos para la concesión, se denegará la patente.

Se invita al solicitante se sirva indicar, si así lo considera, su renuncia al término faltante de sesenta (60) días para dar respuesta a este requerimiento y presentarla por escrito.

Finalmente, se le recuerda al solicitante que si como respuesta a este requerimiento llegara a modificar el capítulo reivindicatorio y éste contenga más de diez (10) reivindicaciones, no pagará la tasa de modificación voluntaria pero sí la correspondiente al pago por reivindicación adicional.

Notifíquese el presente oficio conforme a lo dispuesto en el numeral 5.2, literal e), del capítulo quinto del título primero de la Circular Única No. 10 de 2001.

JOSÉ LUIS SALAZAR LÓPEZ
Director de Nuevas Creaciones (c)

El anterior requerimiento fue notificado por fijación en lista, de fecha 2015-09-15

Elaboró: Mario Andres Forero
Revisó: Dayron Alexander Ramirez Reyes

INFORME DE BÙSQUEDA DE PATENTES PARA EL Radicado N° 14-98853-00007-0000	
CRITERIOS PARA LA BÙSQUEDA (anexar pantallazo o reporte en PDF, junto con los boleanos utilizados)	
Palabras clave utilizadas	Enzimas lisosomales, N-acetil-alfa-D-glucosaminidasa (NaGlu), Composición+ and NaGlu, enfermedad autosómica recesiva, síndrome de Sanfilippo de tipo B, receptor manosa-6-fosfato (M6P)
CLASIFICACIONES INTERNACIONALES UTILIZADAS PARA LA BÚSQUEDA	A61K38/47; C12N5/07; C12N9/26

BASES DE DATOS CONSULTADAS.

Patentscope	Google/patents		
NCBI	PatBase		
Espacenet	Epoquenet		
Lens	Sciencedirect		

INFORMES DE EXÁMENES REALIZADOS EN OTRAS OFICINAS (documentos patentes, literatura no patente etc…)

Oficina	Fecha del examen o de reporte de búsqueda de documentos	Anterioridades encontradas para el examen o reportados en el examen de búsqueda(relacionarlos todos)	Reiv. afectadas	RELEVANCIA (requisito que afecta)	FUERON TENIDOS EN CUENTA PARA EL EXAMEN EN LA OFICINA COLOMBIANA	
					SI	NO
EUROPEAN SEARCH REPORT EPO	27/Mayo/2015	Di Natale P et al., 2005. Treatment of the mouse model of mucopolysaccharidosis type IIIB with lentiviral-NAGLU vector.	1 - 27	Nivel inventivo	X	
		Zhao H. G. *et al.,* 1996. The molecular basis of Sanfilippo síndrome type B.	1 - 27	Nivel inventivo		X
		Weber B. *et al.,* 2001. Expression and characterization of human recombinant and alpha - N – actylglucosaminidase.	1 - 27	Nivel inventivo		X
		WO2011/163652	1 - 27	Documento Y, P		X
		US2012/021436	1 - 27	Documento Y, P		X

DOCUMENTOS ADICIONALES ENCONTRADOS POR EL EXAMINADOR DE ACUERDO A LOS CRITERIOS DE BÙSQUEDA.

WO2009/131698
WO2011163652
US2012003202
P Kim *et al.,* 2009. Carbohydrate recognition by the mannose-6-phosphate receptors
Schmidtchen A. *et al.,* 1998. NAGLU Mutations Underlying Sanfilippo Syndrome Type B
Champion K. *el al.,* 2010. Identification and characterization of a novel homozygous deletion in the a-N-acetylglucosaminidase gene in a patient with Sanfilippo type B síndrome (mucopolysaccharidosis IIIB)
US2006247177
US2006247177
US2011223147
CN104131094

BÚSQUEDA DE SECUENCIAS
Número de depósito / patente y N° de secuencia
% de identidad

SEQ ID NO (de la solicitud)	NCBI	The Lens	EMBL-EBI	DDJB	Genome Quest
SEQ ID NO: 1	SEQ ID: refINP 000254.2 presenta un 100% de identidad				

Búsqueda de Secuencias

alpha-N-acetylglucosaminidase precursor [Homo sapiens]

Sequence ID: ref|NP_000254.2| **Length:** 743 **Number of Matches:** 1

▸ See 1 more title(s)

Range 1: 1 to 743 GenPept Graphics ▼ Next Match ▲ Previous Match

Score	Expect	Identities	Positives	Gaps
2489 bits(5651)	0.0	743/743(100%)	743/743(100%)	0/743(0%)

```
Query  1    MEAVAVAAAVGVLLLAGAGGAAGDEAREAAAVRALVARLLGPGPAADFSVSVERALAAKP  60
            MEAVAVAAAVGVLLLAGAGGAAGDEAREAAAVRALVARLLGPGPAADFSVSVERALAAKP
Sbjct  1    MEAVAVAAAVGVLLLAGAGGAAGDEAREAAAVRALVARLLGPGPAADFSVSVERALAAKP  60

Query  61   GLDTYSLGGGGAARVRVRGSTGVAAAAGLHRYLRDFCGCHVAWSGSQLRLPRPLPAVPGE  120
            GLDTYSLGGGGAARVRVRGSTGVAAAAGLHRYLRDFCGCHVAWSGSQLRLPRPLPAVPGE
Sbjct  61   GLDTYSLGGGGAARVRVRGSTGVAAAAGLHRYLRDFCGCHVAWSGSQLRLPRPLPAVPGE  120

Query  121  LTEATPNRYRYYQNVCTQSYSFVWWDWARWEREIDWMALNGINLALAWSGQEAIWQRVYL  180
            LTEATPNRYRYYQNVCTQSYSFVWWDWARWEREIDWMALNGINLALAWSGQEAIWQRVYL
Sbjct  121  LTEATPNRYRYYQNVCTQSYSFVWWDWARWEREIDWMALNGINLALAWSGQEAIWQRVYL  180

Query  181  ALGLTQAEINEFFTGPAFLAWGRMGNLHTWDGPLPPSWHIKQLYLQHRVLDQMRSFGMTP  240
            ALGLTQAEINEFFTGPAFLAWGRMGNLHTWDGPLPPSWHIKQLYLQHRVLDQMRSFGMTP
Sbjct  181  ALGLTQAEINEFFTGPAFLAWGRMGNLHTWDGPLPPSWHIKQLYLQHRVLDQMRSFGMTP  240

Query  241  VLPAFAGHVPEAVTRVFPQVNVTKMGSWGHFNCSYSCSFLLAPEDPIFPIIGSLFLRELI  300
            VLPAFAGHVPEAVTRVFPQVNVTKMGSWGHFNCSYSCSFLLAPEDPIFPIIGSLFLRELI
Sbjct  241  VLPAFAGHVPEAVTRVFPQVNVTKMGSWGHFNCSYSCSFLLAPEDPIFPIIGSLFLRELI  300

Query  301  KEFGTDHIYGADTFNEMQPPSSEPSYLAAATTAVYEAMTAVDTEAVWLLQGWLFQHQPQF  360
            KEFGTDHIYGADTFNEMQPPSSEPSYLAAATTAVYEAMTAVDTEAVWLLQGWLFQHQPQF
Sbjct  301  KEFGTDHIYGADTFNEMQPPSSEPSYLAAATTAVYEAMTAVDTEAVWLLQGWLFQHQPQF  360

Query  361  WGPAQIRAVLGAVPRGRLLVLDLFAESQPVYTRTASFQGQPFIWCMLHNFGGNHGLFGAL  420
            WGPAQIRAVLGAVPRGRLLVLDLFAESQPVYTRTASFQGQPFIWCMLHNFGGNHGLFGAL
Sbjct  361  WGPAQIRAVLGAVPRGRLLVLDLFAESQPVYTRTASFQGQPFIWCMLHNFGGNHGLFGAL  420

Query  421  EAVNGGPEAARLFPNSTMVGTGMAPEGISQNEVVYSLMAELGWRKDPVPDLAAWVTSFAA  480
            EAVNGGPEAARLFPNSTMVGTGMAPEGISQNEVVYSLMAELGWRKDPVPDLAAWVTSFAA
Sbjct  421  EAVNGGPEAARLFPNSTMVGTGMAPEGISQNEVVYSLMAELGWRKDPVPDLAAWVTSFAA  480

Query  481  RRYGVSHPDAGAAWRLLLRSVYNCSGEACRGHNRSPLVRRPSLQMNTSIWYNRSDVFEAW  540
            RRYGVSHPDAGAAWRLLLRSVYNCSGEACRGHNRSPLVRRPSLQMNTSIWYNRSDVFEAW
Sbjct  481  RRYGVSHPDAGAAWRLLLRSVYNCSGEACRGHNRSPLVRRPSLQMNTSIWYNRSDVFEAW  540

Query  541  RLLLTSAPSLATSPAFRYDLLDLTRQAVQELVSLYYEEARSAYLSKELASLLRAGGVLAY  600
            RLLLTSAPSLATSPAFRYDLLDLTRQAVQELVSLYYEEARSAYLSKELASLLRAGGVLAY
Sbjct  541  RLLLTSAPSLATSPAFRYDLLDLTRQAVQELVSLYYEEARSAYLSKELASLLRAGGVLAY  600

Query  601  ELLPALDEVLASDSRFLLGSWLEQARAAAVSEAEADFYEQNSRYQLTLWGPEGNILDYAN  660
            ELLPALDEVLASDSRFLLGSWLEQARAAAVSEAEADFYEQNSRYQLTLWGPEGNILDYAN
Sbjct  601  ELLPALDEVLASDSRFLLGSWLEQARAAAVSEAEADFYEQNSRYQLTLWGPEGNILDYAN  660

Query  661  KQLAGLVANYYTPRWRLFLEALVDSVAQGIPFQQHQFDKNVFQLEQAFVLSKQRYPSQPR  720
            KQLAGLVANYYTPRWRLFLEALVDSVAQGIPFQQHQFDKNVFQLEQAFVLSKQRYPSQPR
Sbjct  661  KQLAGLVANYYTPRWRLFLEALVDSVAQGIPFQQHQFDKNVFQLEQAFVLSKQRYPSQPR  720

Query  721  GDTVDLAKKIFLKYYPRWVAGSW  743
            GDTVDLAKKIFLKYYPRWVAGSW
Sbjct  721  GDTVDLAKKIFLKYYPRWVAGSW  743
```

Búsqueda en PatBase

7) Family number: 43925953 (WO09131698A2)

Title: PHOSPHORYLATED RECOMBINANT N-ACETYL-ALPHA-D- GLUCOSAMINIDASE (**NAGLU**) AND USES THEREOF

Abstract: The present invention relates generally to phosphorylated recombinant NaGIu fusion proteins, the production of phosphorylated recombinant NaGIu fusion proteins and uses thereof.
Classifications:
International (IPC 8-9): A61K38/47 C07K14/435 (Advanced/Invention); A61K38/43 C07K14/435 (Core/Invention)
CPC: C12N9/16 C12Y301/04045 C07K14/775 A61K38/00 C07K2319/00 C07K2319/02 C12Y302/0105
European: C07K14/775 C12N9/24 C12Y302/01050 K61K38/00 M07K319/00 M07K319/02

8) Family number: 43959995 (US2011223147A)

Title: LYSOSOMAL TARGETING PEPTIDES AND USES THEREOF

Abstract: Source: US2011223147A The present invention provides further improved **compositions** and methods for efficient lysosomal targeting based on the GILT technology. Among other things, the present invention provides methods and **compositions** for targeting lysosomal enzymes to lysosomes using furin-resistant lysosomal targeting peptides. The present invention also provides methods and **compositions** for targeting lysosomal enzymes to lysosomes using a lysosomal targeting peptide that has reduced or diminished binding affinity for the insulin receptor.
Classifications:
International (IPC 8-9): A61K A61K38/00 A61K38/27 A61K38/43 A61K38/46 A61K38/47 A61P3/00 A61P43/00 C07H21/00 C07K1/00 C07K14/47 C07K14/475 C07K14/62 C07K14/65 C07K19/00 C12N1/00 C12N1/15 C12N1/19 C12N1/21 C12N15/09 C12N15/17 C12N15/56 C12N15/62 C12N5/10 C12N9/24 C12N9/26 C12N9/96 C12P21/00 (Advanced/Invention);
C07K14/435 C07K19/00 (Core/Invention);
C07K (Subclass/Invention)
CPC: C12N9/2408 C12Y302/0102 C07K14/65 C07K2319/06
European: C07K14/65 M07K319/06
US: 424/94.3 424/94.300P 424/94.61 424/94.610P 435/188 435/188S 435/200 435/200S 435/201 435/243 435/243S 435/325 435/325S 435/352 435/357 435/360 435/364 435/365.1 435/366 435/367 435/369 435/419 435/419S 514/17.5 530/350 536/23.2 536/23.200S

17) Family number: 57719982 (CN104131094A)

Title: PRIMER **COMPOSITION** FOR LYSOSOMAL DISEASE GENE SCREENING AND KIT USING THE SAME

Abstract: Source: CN104131094A The invention provides a primer **composition** for lysosomal disease gene screening and a kit using the same. The primer **composition** comprises multiple primer sequences respectively aiming at non-repetitive regions of IDUA, ARSB, MAN2B1, ST3GAL5, SMPD1, CTNS, MFSD8, IDS, GUSB, GBA, ARSA, GNPTAB, SLC17A5, CLN8, SGSH, HYAL1, PSAP, GNPTAG, PPT1, CTSD, **NAGLU**, FUCA1, GLB1, SUMF1, MCOLN1, TPP1, HGSNAT, NAGA, GM2A, GALC, LIPA, CLN3, GALNS, NEU1, HEXA, GLA, NPC1, CLN5, MANBA, HEXB, ASAH1, NPC2 and CLN6 genes.
Classifications:
International (IPC 8-9): C12N15/11 C12Q1/68 (Advanced/Invention)
CPC: C12Q1/6883

Family:

Publication number	Publication date	Application number	Application date
CN104131094 A	20141105	CN201410359940	20140725

Priority:
CN201410359940 20140725

Probable Assignee: FENG ZHICHUN
Assignee(s): (std): FENG ZHICHUN
Assignee(s): PURE SEALS
Inventor(s): (std): FENG ZHICHUN ; WANG YAN ; YANG YAO

Búsqueda en EPOQUENET

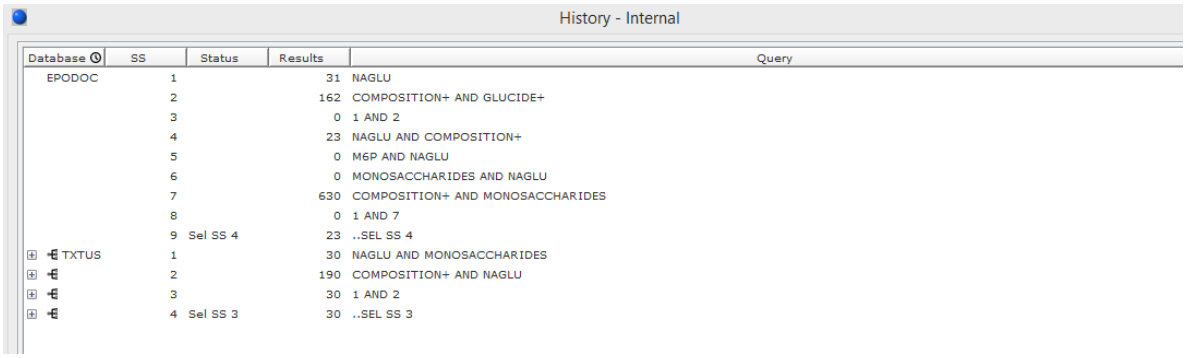

Database	SS	Status	Results	Query
EPODOC	1		31	NAGLU
	2		162	COMPOSITION+ AND GLUCIDE+
	3		0	1 AND 2
	4		23	NAGLU AND COMPOSITION+
	5		0	M6P AND NAGLU
	6		0	MONOSACCHARIDES AND NAGLU
	7		630	COMPOSITION+ AND MONOSACCHARIDES
	8		0	1 AND 7
	9	Sel SS 4	23	..SEL SS 4
TXTUS	1		30	NAGLU AND MONOSACCHARIDES
	2		190	COMPOSITION+ AND NAGLU
	3		30	1 AND 2
	4	Sel SS 3	30	..SEL SS 3

Treatment of the mouse model of mucopolysaccharidosis type IIIB with lentiviral-NAGLU vector

Paola DI NATALE*[1], Carmela DI DOMENICO*, Nadia GARGIULO*, Sigismondo CASTALDO†, Enrico GONZALEZ Y REYERO†, Pratibha MITHBAOKAR‡, Mario DE FELICE‡, Antonia FOLLENZI§, Luigi NALDINI§ and Guglielmo R. D. VILLANI*

*Department of Biochemistry and Medical Biotechnologies, University of Naples Federico II, Via S. Pansini n. 5, 80131 Naples, Italy, †Center for Animal Experimentation, Cardarelli Hospital, Naples, Italy, ‡Stazione Zoologica Anton Dohrn, Naples, Italy, and §HSR-Telethon Institute for Gene Therapy, H. San Raffaele Scientific Institute, Milan, Italy

The Sanfilippo syndrome type B (mucopolysaccharidosis IIIB) is an autosomal recessive disorder due to mutations in the gene encoding NAGLU (α-*N*-acetylglucosaminidase), one of the enzymes required for the degradation of the GAG (glycosaminoglycan) heparan sulphate. No therapy exists for affected patients. We have shown previously the efficacy of lentiviral-NAGLU-mediated gene transfer in correcting *in vitro* the defect on fibroblasts of patients. In the present study, we tested the therapy *in vivo* on a knockout mouse model using intravenous injections. Mice (8–10 weeks old) were injected with one of the lentiviral doses through the tail vein and analysed 1 month after treatment. A single injection of lentiviral-NAGLU vector resulted in transgene expression in liver, spleen, lung and heart of treated mice, with the highest level reached in liver and spleen. Expression of 1 % normal NAGLU activity in liver resulted in a 77 % decrease in the GAG content; more remarkably, an expression of 0.16 % normal activity in lung was capable of decreasing the GAG level by 29 %. Long-term (6 months) follow up of the gene therapy revealed that the viral genome integration persisted in the target tissues, although the real-time PCR analysis showed a decrease in the vector DNA content with time. Interestingly, the decrease in GAG levels was maintained in liver, spleen, lung and heart of treated mice. These results show the promising potential and the limitations of lentiviral-NAGLU vector to deliver the human NAGLU gene *in vivo*.

Key words: gene therapy, glycosaminoglycan, lentiviral vector, mouse model, α-*N*-acetylglucosaminidase, Sanfilippo type B.

INTRODUCTION

Sanfilippo syndrome type B [MPS (mucopolysaccharidosis) IIIB] is an autosomal recessive disorder due to mutations in the gene encoding NAGLU (α-*N*-acetylglucosaminidase; EC 3.2.1.50), one of the enzymes required for the degradation of heparan sulphate [1]. It is heterogeneous at the molecular level, with more than 80 mutations of the NAGLU gene already described in [2–6]. The enzyme defect results in the accumulation of heparan sulphate in the tissues of affected subjects and its abnormal urinary excretion. Affected children are usually diagnosed at 2–8 years of age and they present with sleep disorders, hepatosplenomegaly, hirsutism, vasomotor instability, dysmorphism, dysostosis, delayed development and mental retardation progressing throughout childhood; death occurs, typically, during the 2nd or 3rd decade of life, although patients with a more attenuated phenotype have been reported [7,8].

At present, there is no definite treatment for MPS IIIB [1]. The development of a knockout mouse model of the disease [9], showing a biochemical phenotype generally similar to that of the human disorder, provides a good model for the development of new treatments. This model was used to evaluate the potential of enzyme replacement therapy based on an unphosphorylated form of recombinant NAGLU [10] to verify the efficacy of intracranial injections of adeno-associated vectors for the correction of the neurological impairment [11] and, more recently, to test the therapeutic effect of retrovirally transduced bone marrow [12].

A number of viral vectors have been used in the last few years for gene therapy of lysosomal disorders; more recently, lentiviral vectors were shown to be effective by intracranial delivery into murine models of metachromatic leukodystrophy [13] and MPS VII, β-glucuronidase deficiency [14–16]. Recently, we demonstrated that fibroblasts from patients with MPS IIIB or MPS I, infected with lentiviral vectors, produced consistent levels of a correctly processed protein whose expression is time-persistent and sufficient to reverse abnormal GAG (glycosaminoglycan) accumulation [17,18]. In the present study, we used this late-generation lentiviral vector containing the human NAGLU cDNA driven by a CMV (cytomegalovirus) promoter for the *in vivo* transduction of the therapeutic gene into the murine MPS IIIB model by intravenous administration.

MATERIALS AND METHODS

Materials

Tissue culture reagents and fetal bovine serum were purchased from Sigma (Milan, Italy) and the 4-methylumbelliferyl substrates from Calbiochem (San Diego, CA, U.S.A.). Alcian Blue, heparan sulphate, Protein A-acrylic beads, *p*-nitrophenyl phosphate, alkaline phosphatase-labelled goat anti-mouse Ig were obtained from Sigma. Reagents for immunostaining, including Vecstatin Elite ABC reagent, peroxidase substrate solution and biotinylated rabbit IgG were obtained from Vector Laboratories (Burlingame, CA, U.S.A.). For the standard PCRs, the buffer was obtained from PerkinElmer Life Sciences (Milan, Italy), *Taq* polymerase from Invitrogen SRL (Milan, Italy), dNTPs from Amersham Biosciences (Milan, Italy) and primers from PRIMM (Milan, Italy). Probes and master mix for real-time quantitative PCR were obtained from Applied Biosystems (Milan, Italy).

Abbreviations used: CMV, cytomegalovirus; GAG, glycosaminoglycan; GFP, green fluorescent protein; MPS, mucopolysaccharidosis; NAGLU, α-*N*-acetylglucosaminidase.

[1] To whom correspondence should be addressed (email dinatale@unina.it).

Methods

Large-scale vector production and assays

Lentiviral vector containing the human NAGLU cDNA was prepared as described previously [17,19,20]. For the large-scale preparation, 5×10^6 293T cells/dish were seeded in 24 dishes 6 h before transfection. A total of 22.5 μg of plasmid DNA was used for the quadritransfection of one dish: 10 μg of the transfer vector plasmid pRRLsin.PPT.CMV.NAGLU.WPRE (PPT stands for polypurine tract and termination sequences from *pol* of HIV-1-enhancing nuclear translocation and WPRE for the post-transcriptional regulatory element from the woodchuck hepatitis virus), 6.5 μg of the packaging plasmid pMDLg/pRRE, 2.5 μg of pRSV-Rev construct and 3.5 μg of the envelope plasmid pMD2.G. The viral content was determined by immunocapture of HIV-1 p24 antigen using the HIV-1 p24 core Profile ELISA kit from NEN (Cologno Monzese, Italy). For each large-scale preparation of lentiviral-NAGLU vector, transfection of 1.2×10^8 293T cells yielded 8–20 μg of HIV-1 p24 antigen. To test the viral preparation, 50 ng of p24 was used to infect 10^5 defective fibroblasts in 6 cm plates. Transduction of deficient fibroblasts with each preparation resulted in a mean enzymatic activity of 60.4 ± 23.1 nmol $\cdot$ h^{-1} $\cdot$ (mg of protein)$^{-1}$ (over the range 38.4–84.4); untreated fibroblasts showed a mean activity of 0.33 ± 0.17 (over the range 0.18–0.61).

Transduction efficiency *in vivo*, as measured by using similar doses of a lentiviral vector expressing the GFP (green fluorescent protein) gene, was reported to reach up to 21 % efficiency of GFP-positive cells found in the liver of treated mice [20].

Experimental animals: genotyping

The mouse model of MPS IIIB was created by targeted disruption of exon 6 of the corresponding mouse NAGLU gene [9]. The biochemical phenotype of mutant mice is generally similar to that of the human disorder, the only exception being that affected mice do not show increased urinary excretion of heparan sulphate. The animal studies were approved by the Italian Ministry of Public Health. The mice were genotyped by polymerase reaction analysis performed on DNA samples extracted from tail clipping exactly 1 month after birth. PCRs were performed in a total volume of 100 μl containing 500 ng of template DNA extracted from tail clipping, 1×PCR buffer from PerkinElmer, 0.2 μM of each dNTP, 2.5 units of *Taq* polymerase and two sets of the following primers (0.5 μM each): (i) MXXDe1F, sense primer starting at position 6773 of the murine NAGLU gene, GenBank® accession number AF003255 (5′-GCTCCTACTC-AGAAGTGTCTACAACTGCTC-3′), and MXXDelR, antisense primer starting at position 7279 (5′-GAGGCTGGTAGTAATC-AGCCACCAGTCCTG-3′). Amplification yielded a 537 bp fragment in the presence of the normal allele, no band in the presence of the mutant allele; (ii) Neo1F, sense primer starting at position 202 in the Neo ORF (5′-GTGGCTGGCCACGACG-GGCGTTCCTTGCG-3′), and M7R, antisense primer starting at position 7454 of the murine NAGLU gene (5′-GAGGAA-GATCTTCTTGGAGAGGTCCACGGTG-3′). Amplification yielded no band in the presence of the normal allele but yielded a 1200 bp band in the presence of the mutant allele. Cycling conditions were the following: 96 °C for 5 min, 35 cycles at 95 °C for 45 s, 64 °C for 35 s and 72 °C for 2 min.

In vivo gene therapy: intravenous injections of lentiviral-NAGLU vector

Homozygous mutant mice (8–10 weeks old) obtained from heterozygote matings were used for all *in vivo* transduction experiments. A volume of 200–300 μl of vector in PBS was injected into the tail vein; controls were mock-injected. At the time of killing, the mice were killed with CO_2 and the organs (brain, liver, spleen, lung, heart, thymus and kidney) were removed and immediately frozen in liquid nitrogen or subdivided into parts, one of which was fixed in 4 % (w/v) paraformaldehyde overnight and treated for immunohistochemistry as described in the next paragraph.

NAGLU and lysosomal enzyme assays

For the enzyme assays, 30 mg of the tissue was homogenized in 1 ml of 0.9 % NaCl/0.2 % Triton X-100, rotated for 2 h at 4 °C and centrifuged to remove the debris. NAGLU activity was measured as described in [21]: 50–100 μg of each lysate was added in duplicate to a solution containing 2 mM 4-methylumbelliferyl-NAGLU in 0.2 M sodium acetate buffer (pH 4.3). The cleaved substrate was quantified after a 17 h incubation at 37 °C, and subsequent to the addition of glycine buffer (pH 10.5). Other lysosomal enzyme activities were determined by the method of Li et al. [9] by using 4-methylumbelliferyl substrates incubated with the appropriate amount of homogenate for 1 h at 37 °C under the following conditions: α-L-iduronidase, 10 μl of homogenate with 10 μl of 2 mM substrate in 0.1 M formate (pH 3.2); β-glucuronidase, 50 μl of homogenate with 50 μl of 0.2 mM substrate in 0.1 M sodium acetate buffer (pH 4.3); β-hexosaminidase, 25 μl of homogenate with 125 μl of 0.24 mM substrate in 0.1 M sodium acetate buffer (pH 5). The amount of fluorescent product released in the enzyme reaction was determined from a standard curve using 4-methylumbelliferone.

Analysis of GAG (quantitative determination)

Soluble GAGs were precipitated from tissue homogenates with Alcian Blue for quantitative measurement [9,22]. The mice were killed and organs were dissected as described above. Frozen tissues were freeze-dried and, after weighing, resuspended in 0.9 % NaCl/0.2 % Triton X-100 (30 μl/mg dry weight), rotated at 4 °C overnight and centrifuged to remove the debris. GAGs were precipitated with Alcian Blue, the blue precipitate was dissolved, and absorbance was measured at 600 nm. Heparan sulphate from porcine intestinal mucosa was used as standard.

Immunohistochemistry

An enzyme-based immunohistochemical stain was used to detect the human NAGLU in cryosections of liver after viral treatment. For antibody staining of recombinant NAGLU, the liver was fixed overnight in 4 % paraformaldehyde and embedded in paraffin. Sections (6 μm thick), deparaffinized and rehydrated, were incubated with Protein A-purified anti-human NAGLU and biotinylated anti-rabbit antibody. Colour was developed using the ABC Elite Vector Staining kit and the horseradish peroxidase substrate by VIP kit. The presence of recombinant NAGLU was visualized by the magenta colour of the peroxidase reaction [10].

Biodistribution of viral genome: PCR assay

Genomic DNA for the PCR assay was purified from tissue homogenates by phenol–chloroform extraction and ethanol precipitation. The integrity of the DNA was verified by performing, for all the tissues, a PCR amplification with Neo1F and M7R primers (described in the Experimental animals: genotyping subsection). The extracted DNA was then subjected to PCR in a total volume of 100 μl containing 1× buffer, 0.2 mM of each dNTP and 0.5 μM each of the forward and reverse primers NB17 and NB18 [2]. These primers were selected to amplify a 429 bp fragment from exon 6 of the human NAGLU gene that is present

Table 1 Dose–response after the intravenous injection of lentiviral-NAGLU vector in MPS IIIB mice

MPS IIIB mice (8–10 weeks old) were intravenously injected with a lentiviral-NAGLU vector at the indicated p24 doses for each mouse. Normal and heterozygous mice were mock-injected. After 1 month, mice were killed and tissues were analysed for NAGLU activity. Enzyme activity values represent the means ± S.D. for three animals. *$P < 0.05$ versus untreated mice; no symbol is used to indicate $P > 0.05$.

	NAGLU activity [nmol · (17 h)$^{-1}$ · (mg of protein)$^{-1}$]						
Lentiviral dose (μg of p24)	Liver	Spleen	Lung	Thymus	Heart	Kidney	Brain
0	0.020 ± 0.023	0.050 ± 0.026	0.039 ± 0.023	0.023 ± 0.018	0.024 ± 0.016	0.027 ± 0.005	0.04 ± 0.0028
3	0.055 ± 0.037	0.070 ± 0.033	0.073 ± 0.025	0.046 ± 0.028	0.061 ± 0.030	0.049 ± 0.034	0.041 ± 0.037
6	0.095 ± 0.037*	0.107 ± 0.020*	0.070 ± 0.018	0.022 ± 0.015	0.082 ± 0.046	0.026 ± 0.024	0.021 ± 0.018
9	0.133 ± 0.045*	0.237 ± 0.08*	0.080 ± 0.016	0.052 ± 0.020	0.080 ± 0.043	0.016 ± 0.010	0.01 ± 0.008
12	2.62 ± 1.6*	32.5 ± 21.3*	0.168 ± 0.057*	0.079 ± 0.060	0.087 ± 0.029*	0.075 ± 0.038	0.045 ± 0.034
Normal mice	228.9 ± 105	117.3 ± 57	106.3 ± 41.6	53.3 ± 15.4	12.4 ± 2.86	76.8 ± 50.5	19.1 ± 2.27
Heterozygous mice	84.8 ± 49	24.5 ± 4.8	69.1 ± 39	33.9 ± 2.8	9.3 ± 2.4	22.7 ± 1	11.8 ± 2.6

only in the affected mice after lentiviral treatment but is absent from the genome of affected untreated mice. The PCR procedure required a 5 min initial denaturation step (96 °C), followed by 35 cycles at 95 °C for 45 s, 54 °C for 35 s and 72 °C for 2 min. The number of cycles was adjusted to obtain a non-saturating range of amplification of vector DNA.

Integration of the lentiviral construct: B2-PCR assay

DNA extracted from mice tissues was subjected to B2-PCR. In a first set of amplifications, primers based on the murine B2 family of highly repeated dispersed elements [23–25] were used together with primers derived from the 5′- or 3′-end of the vector. Reactions were performed on 100 ng of genomic DNA in a 100 μl total volume containing 1× buffer (PerkinElmer), 0.4 mM of each dNTP, 0.8 μM each of the forward and reverse primers, 5 % (v/v) DMSO and 5 units of *Taq* polymerase. Two different primer pairs were used; one at the 5′-end and the other at the 3′-end of the vector genome [20]. The primers for the 5′-end were B2 sense and 5NC2 antisense; the other pairs at the 3′-end were B2 antisense and WPRE sense. After the first amplification, a nested PCR was performed using 10 μl of the first PCR product in a 100 μl final volume using two different internal primers in the vector genome. For the 5′-nested PCR, the primers were LTR9 (sense) and U5PBS (antisense). For the 3′-nested PCR, the primers used were Δnef (sense) and LTR8 (antisense) [20]. As the control, a nested PCR was performed using 10 ng of non-amplified genomic DNA from mice tissues.

Quantitative real-time PCR

Real-time PCR was performed on genomic DNA extracted from the liver and spleen of the 12 μg-injected mice 1 month after treatment and 6 months after treatment. Primers (forward primer: 5′-TGAAAGCGAAAGGGAAACCA-3′; reverse primers: 5′-CCGTGCGCGCTTCAG-3′) and the TaqMan probe (5′-VIC-AGCTCTCTCGACGCAGGACTCGGC-TAMRA-3′) targeted the lentiviral 5′-untranslated region. Amplicon size was 65 bp. Each reaction contained 1× TaqMan universal PCR master mix, 400 nM of each primer, 200 nM TaqMan probe and 300 ng of sample DNA in a final volume of 25 μl. As standard, the diluted gene transfer vector was used (from 1×10^6 copies to 1 copy/reaction in GeneAmp 1× PCR buffer containing 20 ng/μl sheared salmon sperm DNA). The following cycling parameters were used: 2 min incubation at 50 °C followed by 10 min at 95 °C and 40 cycles of denaturation at 95 °C for 15 s and annealing/extension at 60 °C for 1 min. All the reactions were performed in triplicate sets and the results were reported as the average of three reactions. Real-time PCR targeted for the mouse β-actin gene was used for normalization of the DNA content; for this purpose, a β-actin-specific TaqMan probe was used (5′-VIC-CACTGCCGCATCCTCTTCCTCCC-TAMRA-3′) and the following primers were employed: forward primer 5′-AGAG-GGAAATCGTGCGTGAC-3′ and reverse primer 5′-CAATAG-TGACCTGGCCGT-3′. To obtain the vector copy number for each cell, the values were divided by the number of cells corresponding to 300 ng of genomic mouse DNA.

Transgene-specific immune response: ELISA

The presence of an immune response in mice against human NAGLU was evaluated by an ELISA of samples from affected mice after lentiviral-NAGLU treatment. For the detection of anti-NAGLU antibodies, the wells were coated with 0.2 μg of recombinant NAGLU in 50 μl of PBS (pH 5.8) and blocked with 0.1 % Tween 20 in PBS. Serum samples from mice treated with lentiviral-NAGLU vector and untreated controls were diluted in PBS; after primary antibody binding, the samples were washed before the addition of the secondary antibody, alkaline phosphatase-labelled goat anti-mouse Ig. After washing, 200 μl of the alkaline phosphatase substrate (*p*-nitrophenyl phosphate) was added and absorbance was measured at 405 nm on a Bio-Rad ELISA reader.

A titration curve was established in the serum of mice killed 1 month after treatment and in the serum of mice killed 6 months after treatment by using several dilutions of mice serum.

RESULTS

In vivo expression of recombinant NAGLU: enzyme activity

Subsets of three affected mice were injected via the tail vein with different doses of lentiviral-NAGLU vector (3, 6, 9 and 12 μg of p24 viral protein) as described in the Materials and methods section. All animals were 8–10 weeks old. Untreated affected mice (Table 1, 0 μg of p24), normal mice and heterozygous mice were mock-treated. Mice were killed 1 month after treatment, and tissues were analysed for NAGLU activity. The results of these experiments are reported in Table 1. As shown in this Table, the NAGLU activity in all organs of untreated mice was nearly zero. In contrast, in animals treated with one of the doses of the vector, a dose–response was observed. At the highest viral dose (12 μg), the liver, spleen, lung and heart of the injected mice showed a significant increase in enzyme activity compared with those of untreated animals, with the highest levels present in the liver and spleen. A NAGLU activity of 2.62 nmol (17 h)$^{-1}$ · (mg of protein)$^{-1}$ was reached in the liver, corresponding to 1.14 % of the normal control; in the spleen, the value of 32.5 nmol

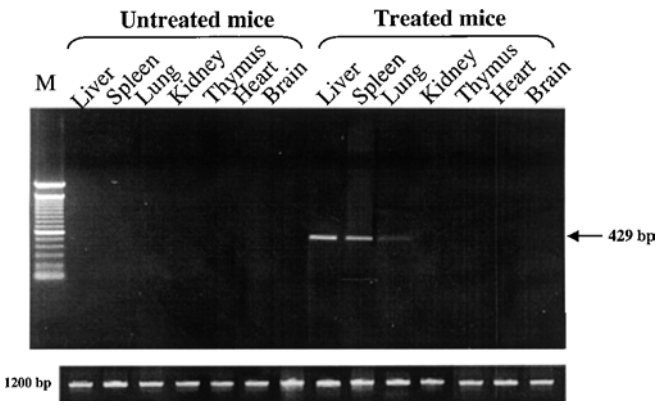

Figure 1 Biodistribution of lentiviral-NAGLU vector in injected mice

MPS IIIB mice were injected with 12 μg of p24 lentiviral dose and killed 1 month after treatment. Biodistribution of the lentiviral gene transfer vector into the mouse genome was evaluated by a single PCR amplification using human NAGLU cDNA-specific primers and genomic DNA extracted from the various tissues. The integrity of the DNA was determined by amplifying a 1200 bp region of the neo-gene belonging to the mutant allele of the MPS IIIB mice (bottom panel).

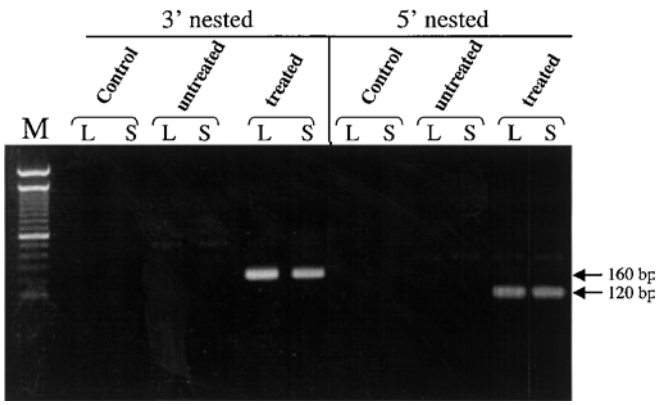

Figure 2 Proviral integration after systemic delivery: nested PCR

To verify the integration of the lentiviral DNA into the host genome, two rounds of PCR were used. A first B2-specific PCR performed on DNA extracted from liver (L) or spleen (S) of 12 μg-injected mice 1 month after treatment was followed by a nested PCR. In the first set of amplifications, primers based on the murine B2 family of highly repeated dispersed elements were used together with primers derived from the 5′- or 3′-end of the vector. Limiting amounts of the amplified products and non-amplified genomic DNA were then used as templates for a second round of PCR using nested primers at the 5′-end (5′-nested) or 3′-end (3′-nested) of the vector. Control, genomic DNA subjected only to nested PCR; L, liver; S, spleen.

$(17\ h)^{-1} \cdot (mg\ of\ protein)^{-1}$ corresponded to 27.7 % of the normal control (Table 1). For the lung and heart, the restored NAGLU activities were less consistent, with the values corresponding to 0.16 and 0.7 % of the values found in normal controls respectively. Lentiviral-NAGLU vector did not mediate recombinant NAGLU expression in the thymus, kidney or brain, the values of the enzyme activity being very similar to those found in untreated animals (Table 1).

Biodistribution and integration of lentiviral-NAGLU vector

To determine the biodistribution of lentiviral-NAGLU vector administered through the tail vein, various organs of the mice were collected 1 month after injection with the 12 μg dose. The presence of the vector genome, as determined by the PCR analysis described in the Materials and methods section, is reported in Figure 1. Lentiviral vector DNA was detected at the highest level in the liver and spleen of injected mice; a much lower level of vector DNA could be detected in the lung, whereas no signal was recovered from the heart, kidney, thymus and brain of the affected mice and from all tissues of the untreated controls. To verify the integration of the vector DNA into the host genome, a double round of PCR amplification was performed on DNA extracted from the liver and spleen of injected and untreated mice. Limiting amounts of the amplified products and non-amplified genomic DNA were used as templates for a second round of PCR using nested primers at the 5′- or 3′-end of the vector genome (Figure 2). As shown in this Figure, the expected bands (160 bp for the 3′-nested PCR and 120 bp for the 5′-nested PCR) were obtained only from the amplified products, indicating that the vector genome was integrated in the mouse DNA.

In vivo expression of recombinant NAGLU: immunohistochemical localization in the liver

To confirm the presence of recombinant NAGLU in the liver tissue from the lentiviral-treated mice, immunohistochemical staining was performed as described under the Materials and methods section. Immunohistochemical staining for NAGLU demonstrated that the recombinant protein was present in the 12 μg-treated mice (Figure 3A), whereas the untreated affected mice had no detectable protein (Figure 3B). The presence of human NAGLU enzyme, visualized by the brown colour of the peroxidase reaction (Figure 3A, arrows), allowed us to estimate that approx. 3–4 % of the liver cells from the treated mice were transduced and that most of them were Kupffer cells, as determined based on their morphology.

Correction of the phenotype after lentiviral treatment: levels of soluble GAG

To study the lentiviral-mediated correction of lysosomal storage in the MPS IIIB affected mice, the GAG dosage was performed on tissues from the 12 μg p24-injected mice. The results are reported in Table 2. As shown in this Table, the GAG content in the injected mice was substantially decreased, corresponding to a decrease of 77 % in the liver, 46 % in the spleen, 29 % in the lung and 16 % in the heart, whereas no effect was found in the kidney or brain (Table 2).

Correction of the phenotype after lentiviral treatment: lysosomal enzyme activity

Since it was reported [9] that the MPS IIIB knockout mouse shows a secondary increase of lysosomal enzyme activity (β-hexosaminidase and β-glucuronidase) both in the liver and brain or only in the liver (α-L-iduronidase), these lysosomal activities were measured in the 12 μg of p24-injected mice 1 month after treatment. We demonstrated that the lentiviral-NAGLU injection was capable of partially decreasing these enzyme activities in the liver tissue (Figure 4), with particular relevance to β-hexosaminidase activity, which reached values very similar to those found in heterozygous mice or in normal mice, resulting in a decrease of approx. 40 %. As expected, no decrease in α-L-iduronidase, β-glucuronidase or β-hexosaminidase activities was observed in the brain of injected mice.

Immune response of mice treated with lentiviral-NAGLU vector

To determine the presence of anti-recombinant NAGLU mouse IgG, blood was collected from the 12 μg-treated mice at different time points. In all the analysed sera (Figure 5A), a humoral response was not detected 1 week post-injection; the levels slightly increased at later time points. At 1 month after treatment, the

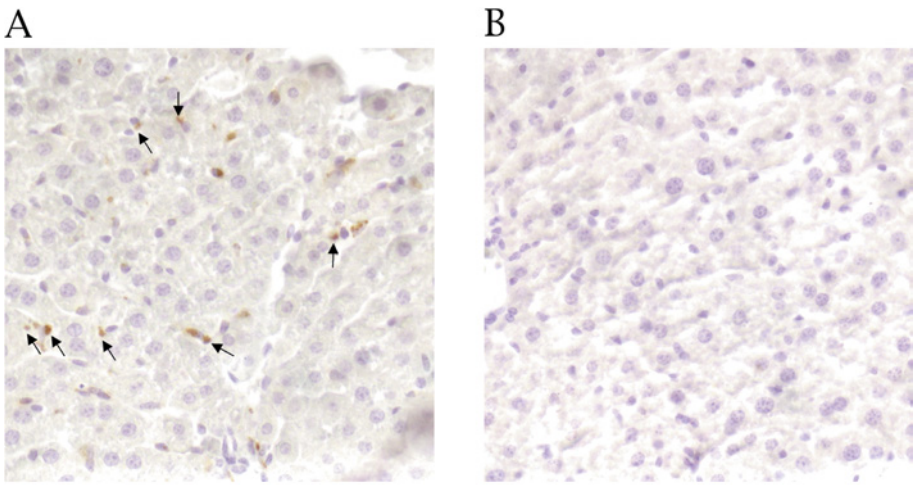

Figure 3 Immunohistochemical localization of recombinant NAGLU in liver

Immunostaining was performed on paraffin-embedded liver sections from a mouse treated with 12 μg of lentiviral vector and killed 1 month later. (**A**) A $\times$40 magnification of the treated mouse; (**B**) the untreated control. The presence of human NAGLU enzyme was visualized by the brown colour of the peroxidase reaction (arrows): most of the positive cells were Kupffer cells. The tissues were counterstained with haematoxylin, which stains the nuclei blue.

Table 2 GAG levels in tissues from lentiviral-NAGLU-treated mice

MPS IIIB mice (8–10 weeks old) were intravenously injected with 12 μg of lentiviral-NAGLU vector corresponding to 0.75×10^9 T.U. (transducing units, calculated as endpoint titre on HeLa cells). Normal and heterozygous mice were injected with PBS. After 1 month, mice were killed and tissues were analysed for the GAG content. Data are means $\pm$ S.D. for three animals. *$P < 0.01$ versus untreated mice; †$P < 0.05$ versus untreated mice; no symbol is used to indicate $P > 0.05$.

	GAG level (μg/mg tissue)					
Mouse	Liver	Spleen	Lung	Heart	Kidney	Brain
Untreated	7.12 $\pm$ 1.09	4.11 $\pm$ 1.0	3.49 $\pm$ 0.44	2.4 $\pm$ 0.15	14.9 $\pm$ 3.27	7.35 $\pm$ 3.0
12 μg-treated	1.67 $\pm$ 0.6*	2.25 $\pm$ 0.27†	2.5 $\pm$ 0.34†	2.0 $\pm$ 0.10†	14.2 $\pm$ 2.27	12.9 $\pm$ 3.28
Normal	0.61 $\pm$ 0.14	1.17 $\pm$ 0.27	0.55 $\pm$ 0.15	1.14 $\pm$ 0.82	0.51 $\pm$ 0.1	2.26 $\pm$ 1.27

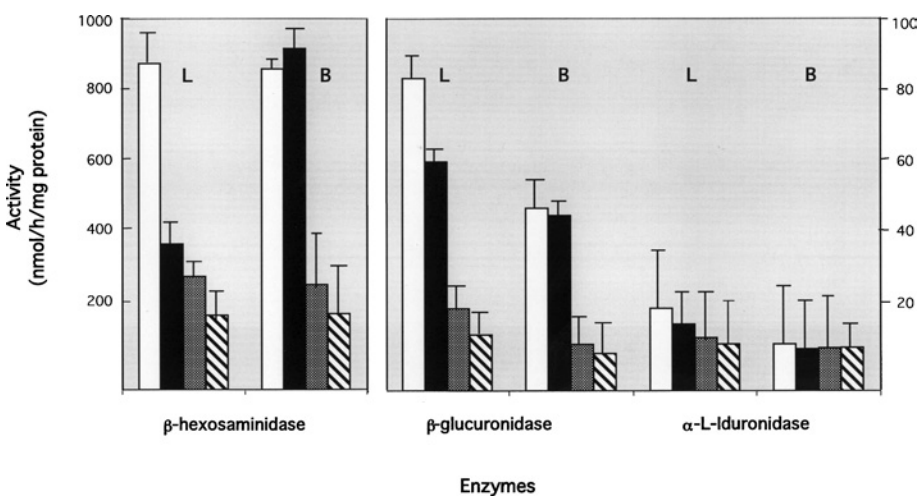

Figure 4 Correction of the phenotype after lentiviral treatment: lysosomal enzyme activities

MPS IIIB mice were injected with 12 μg of p24 viral vector; 1 month later, liver (L) and brain (B) were assayed for lysosomal enzyme activities with fluorimetric assays. Each data point represents the mean $\pm$ S.D. for three mice. Values on the left refer to β-hexosaminidase activity and values on the right to β-glucuronidase and α-L-iduronidase activities. Decrease in β-hexosaminidase was statistically significant at $P = 0.001$; decrease in β-glucuronidase was statistically significant at $P = 0.01$. White bar, untreated mice; black bar, treated mice; dotted bar, heterozygous mice; striped bar, normal mice.

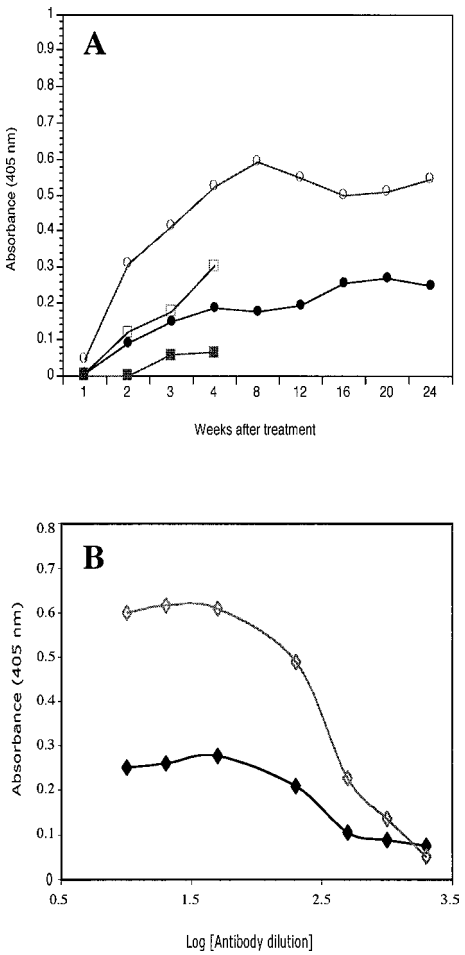

Figure 5 Immune response of mice treated with lentiviral-NAGLU vector

MPS IIIB mice (two for each subset) were intravenously injected with lentiviral-NAGLU vector at the 12 μg dosage and killed 1 month (□) or 6 months (○) after treatment. All values are averages at the indicated time points. (**A**) The anti-NAGLU antibody levels as measured by an ELISA. The mice serum was tested at 1:50 dilution (open symbols) or at 1:500 dilution (closed symbols). (**B**) The titration curves in the serum of mice killed 1 month (◇) or 6 months (◆) after treatment.

antibody titre obtained was very low, with the maximum dilution of antiserum determined to be 50 times (Figure 5B).

Long-term (6 months) follow-up of lentiviral-NAGLU therapy

To evaluate whether a single administration of lentiviral vector into the peripheral blood of the mouse led to a long-term expression of the NAGLU gene, MPS IIIB mice were injected with 12 μg of viral dose and examined after 6 months. Except for the spleen, no significant NAGLU activity was detected in any of the tissues analysed (Table 3); however, a statistically significant decrease in the GAG content was found in the liver, spleen, lung and heart of the injected animals, the decrease being 35, 36, 44 and 34 % respectively (Table 3). B2-PCR analysis revealed the persistence of the viral genome in the liver, spleen and lung of the analysed mice, indicating that the integration of the vector was still present after 6 months (results not shown).

To quantify the amount of integrated vector sequences, a quantitative PCR analysis was performed. The DNA copy number was determined in the liver and spleen by normalizing it to the β-actin sequence of the mouse genome. As shown in Table 4, the vector DNA was much lower in tissues of mice killed 6 months after injection compared with the tissues from animals analysed 1 month after treatment. Interestingly, the decrease in vector DNA was much greater in the liver tissue than in the spleen.

The immune response tests on the sera collected 6 months after treatment showed that the anti-NAGLU humoral response remained at similar levels to those obtained at 1 month after treatment (Figure 5A). At 6 months after treatment, the resulting antibody titre was very low, with the maximum dilution of antiserum determined to be 50 times (Figure 5B).

Table 3 Long-term (6 months) follow up of lentiviral-NAGLU treatment

MPS IIIB mice (8–10 weeks old) were intravenously injected with 12 μg of lentiviral-NAGLU vector. Untreated age-matched controls were mock-injected. After 6 months, mice were killed and tissues analysed for NAGLU activity and GAG content. Data are means ± S.D. for three animals. *$P < 0.05$ versus untreated mice; no symbol is used to indicate $P > 0.05$.

Mouse	Tissue	NAGLU activity [nmol · (17 h)$^{-1}$ · (mg of protein)$^{-1}$]	GAG level (μg/mg tissue)
Untreated	Liver	0.019 ± 0.020	10.0 ± 2.15
	Spleen	0.067 ± 0.018	5.0 ± 0.81
	Lung	0.096 ± 0.027	4.84 ± 0.28
	Heart	0.068 ± 0.020	4.5 ± 0.20
Treated	Liver	0.028 ± 0.011	6.5 ± 0.40*
	Spleen	0.154 ± 0.044*	3.2 ± 0.28*
	Lung	0.115 ± 0.039	2.7 ± 1.09*
	Heart	0.072 ± 0.01	3.0 ± 0.88*

Table 4 Real-time PCR for quantitative assessment of lentiviral-NAGLU vector

Mice were treated with 12 μg of p24 viral protein and killed at two time points after injection (1 and 6 months). Real-time PCR analysis was performed on DNA isolated from the liver and spleen. Copy numbers were obtained from known copies of positive control plasmid diluted into negative control mouse liver DNA. Results are expressed as number of copies/cell.

	Time after treatment	
Tissue	1 month	6 months
Liver	0.21 ± 0.08	0.0071 ± 0.003
Spleen	0.059 ± 0.028	0.0225 ± 0.0092

DISCUSSION

A number of viral vectors have been proposed in the last few years for gene therapy. Among these, lentiviral vectors appear to be promising tools: they integrate a sizeable gene expression cassette efficiently into the target cells, providing for a stable and inherited genetic modification; moreover, they can integrate into the genome of both dividing and non-dividing cells [26]. A third generation lentiviral vector was developed using only a fractional set of HIV genes: *gag*, *pol* and *rev*, with constructs non-functional outside the vector producer cells [19,27,28]. These late generation recombinant lentiviral vectors have significantly improved biosafety but still maintain high transduction efficiency and a broad targeting range; they were shown to be effective by intracranial delivery into murine models of metachromatic leukodystrophy [13] and β-glucuronidase deficiency, MPS VII [14–16].

We used an improved vector construct packaged by a quadri-transfection minimal system where the NAGLU cDNA is driven by the CMV promoter. We recently reported that this vector was

capable of restoring NAGLU enzyme activity and correct the metabolic defect in MPS IIIB-deficient fibroblasts [17].

In this paper, we report our data on lentiviral-NAGLU gene therapy *in vivo* for the murine model of MPS IIIB disease. Our results show that 1 month after a single administration of one of the vector doses, the transgene expression was mainly present in the liver and spleen of treated animals. At the highest viral dose used in the present study, the transgene expression was evident also in the lung and heart. PCR analyses confirmed the presence of vector DNA in the liver, spleen and lung of treated animals, showing higher copy numbers of vector DNA in the liver than in the spleen. These results are in agreement with previous biodistribution studies on intravenous injected lentiviral vectors [20,29].

The dose–response reported in the present study seems to suggest a threshold effect: in both liver and spleen, there was an almost linear response up to 9 μg of viral vector followed by a nonlinear response when the dose was increased to 12 μg. Although this phenomenon was never reported for lentiviral vectors, indeed it was found for adenoviral vectors [30].

In 12 μg-treated mice, the recovered recombinant NAGLU activity ranged from the highest value in the liver (1.1 % of normal) to the lowest value in the lung (0.16 % of normal). It is possible that a limited population of cells (liver Kupffer cells and lung macrophages) stores most of the GAG in this mouse model and that these are the cells that were mainly transduced and corrected. Although minute, the recombinant NAGLU activity resulted in significant decrease of GAG accumulation: it is remarkable, in fact, that 0.16 % of the wild-type NAGLU activity achieved in the lung of treated animals was sufficient to bring a 29 % decrease in GAG level in that tissue. It is possible that complete normalization of GAG accumulation can be reached with higher doses of lentiviral-NAGLU vector, at least in the liver and spleen.

In the liver of treated mice, only 3–4 % of the liver cells appeared to be transduced, as shown by immunohistochemistry tests. This implies that the recombinant NAGLU activity found in liver, which gives rise to the decrease in GAG, is quite probably secreted; the secreted protein is taken up by the untransduced MPS IIIB mouse cells, resulting in the correction of GAG accumulation. The lack of a visible gradient of immunoreactivity around the positive cells could be due to the limitations of the immunohistochemistry technique and not due to a real lack of partially corrected cells. The secretion–recapture mechanism could apply also to the other organs metabolically corrected in the present study, i.e. spleen, lung and heart. Our results are in agreement with recent work on the intravenous administration into immunodeficient mice of lentiviral vectors carrying either an intracellular marker gene (GFP) or a gene of a secreted molecule (Factor IX): high transduction of the liver, spleen and bone marrow was obtained, with levels of Factor IX in the murine plasma (1–2 % of normal) that would be therapeutically useful if achieved in haemophilia B patients [20].

The efficacy of lentiviral gene therapy in the liver was confirmed by the decrease in activity of three lysosomal enzymes: β-hexosaminidase, β-glucuronidase and α-L-iduronidase. This finding is in agreement with the results of Yu et al. [10] that show a decrease in these lysosomal activities after short-term enzyme replacement therapy in MPS IIIB mice. Secondary increases in the lysosomal enzyme activity occur in lysosomal storage diseases, and gene or enzyme therapy often normalize these levels. For the MPS VII murine model, enzyme replacement decreased the increased α-galactosidase, β-galactosidase and β-hexosaminidase activity levels [14] and gene therapy decreased mRNA levels of two lysosomal enzymes in the brain [31]. It is currently unknown whether these secondary changes occur as a result of increased transcription or decreased protein degradation. A recent study [32] on this has suggested that both transcriptional and post-transcriptional mechanisms are involved in the increase in enzyme activity.

In the present study, no correction was obtained in the brain of mice treated with lentiviral-NAGLU vector; this was as expected since intravenous injections cannot cross the blood–brain barrier. Indeed, intracranial injections of viral vectors resulted in neurological correction of lysosomal storage in some murine models [11,13–16,31]. A direct injection of the lentiviral-NAGLU vector is expected to result in the correction of lysosomal storage in MPS IIIB murine brain. However, less invasive procedures based on new technologies to cross the blood–brain barrier need to be developed. In this respect, the use of hyperosmotic drugs [33] or bone marrow stem cells [34] could be alternative avenues of approach. Recently, transplantation of retrovirally transduced bone marrow was reported to have a therapeutic effect on brain of affected MPS IIIB mice [12].

With the same type of lentiviral vector, a widespread transduction of non-parenchymal liver and spleen cells was recently demonstrated, suggesting that antigen-presenting cells were also efficiently transduced by lentiviral vectors [35,36] and probably triggered an immune response to the transgene product. In our case, however, 4 weeks after the 12 μg p24 viral treatment, the anti-NAGLU immune response did not prevent the transgene expression and its distribution to non-transduced cells, as demonstrated by the metabolic correction of GAG accumulation achieved in the liver, spleen, lung and heart.

Long-term (6 months) lentiviral-NAGLU treatment of MPS IIIB mice showed a persistent effect in the liver, spleen, lung and heart. It could well be that, in these tissues, the low level of NAGLU activity recovered after treatment was sufficient to maintain the decreased GAG levels; alternatively, the decreased GAG at 6 months could be due to a very slow rate of reaccumulation of the heparan sulphate. PCR analysis showed that the vector DNA was still integrated in the liver, spleen and lung tissues; however, the DNA copy numbers proved to be halved in the spleen (in agreement with the residual NAGLU activity present in this organ), whereas a more significant decrease was evident in the liver. This could be due to either the turnover of transduced Kupffer cells or the induction of cytotoxic T-lymphocytes, resulting in the clearance of transduced cells. The data on the humoral response obtained after 6 months seem to exclude this hypothesis: the level of anti-NAGLU antibodies was apparently low, not much higher than that obtained 1 month after treatment. In a recent study on GFP and Factor IX driven by CMV in the same lentiviral system, the massive immune response directed against the transgenes was reported to be responsible for a clearance of the transduced cells in long-term treatment; selective targeting of the lentiviral expression to hepatocytes using an albumin promoter limited the immune response to the transgene [36]. Further studies are required to clarify this aspect of lentiviral-NAGLU gene therapy.

In conclusion, our results demonstrate the therapeutic potential of lentiviral-NAGLU vector for the correction of the pathology after intravenous gene therapy. The use of tissue-specific promotors and/or the application of techniques capable of overcoming the blood barrier would result in more effective long-term therapy.

We thank E. F. Neufeld (University of California, Los Angeles, U.S.A.) for the MPS IIIB murine model, recombinant human NAGLU and the rabbit antiserum raised against it. We thank Mrs R. Baldoni for typing this paper. This study was supported by grants from MIUR (Ministero dell'Istruzione, dell'Università e della Ricerca Scientifica) and 'Associazione Italiana Mucopolisaccaridosi e Malattie Affini' to P. DiN.

REFERENCES

1 Neufeld, E. F. and Muenzer, J. (2001) The mucopolysaccharidoses. In The Metabolic and Molecular Bases of Inherited Disease, 8th edn (Scriver, C. R., Beaudet, A. L., Sly, W. S. and Valle, D., eds.), pp. 3421–3452, McGraw-Hill, New York

2 Zhao, H. G., Li, H. H., Bach, G., Schmidtchen, A. and Neufeld, E. F. (1996) The molecular basis of Sanfilippo syndrome type B. Proc. Natl. Acad. Sci. U.S.A. **93**, 6101–6105

3 Schmidtchen, A., Greenberg, D., Zhao, H. G., Li, H. H., Huang, Y., Tieu, P., Zhao, H. Z., Cheng, S., Zhao, Z., Whitley, C. B. et al. (1998) NAGLU mutations underlying Sanfilippo syndrome type B. Am. J. Hum. Genet. **62**, 64–69

4 Weber, B., Guo, X. H., Kleijer, W. J., van de Kamp, J. J. P., Poorthuis, B. J. H. M. and Hopwood, J. J. (1999) Sanfilippo type B syndrome (mucopolysaccharidosis IIIB) allelic heterogeneity corresponds to the wide spectrum of clinical phenotypes. Eur. J. Hum. Genet. **7**, 34–44

5 Tessitore, A., Villani, G. R. D., Di Domenico, C., Filocamo, M., Gatti, R. and Di Natale, P. (2000) Molecular defects in the alpha-N-acetylglucosaminidase gene in Italian Sanfilippo type B patients. Hum. Genet. **107**, 568–576

6 Yogalingam, G. and Hopwood, J. J. (2001) Molecular genetics of mucopolysaccharidosis type IIIA and IIIB: diagnostics, clinical and biological implications. Hum. Mutat. **18**, 264–281

7 Andria, G., Di Natale, P., Del Giudice, E., Strisciuglio, P. and Murino, P. (1969) Sanfilippo B syndrome (MPS III B): mild and severe forms within the same sibship. Clin. Genet. **15**, 500–504

8 Di Natale, P. (1991) Sanfilippo B disease: a re-examination of a particular sibship after 12 years. J. Inherit. Metab. Dis. **14**, 23–28

9 Li, H. H., Yu, W. H., Rozengurt, N., Zhao, H. Z., Lyons, K. M., Anagnostaras, S., Fanselow, M. S., Suzuki, K., Vanier, M. T. and Neufeld, E. F. (1999) Mouse model of Sanfilippo syndrome type B produced by targeted disruption of the gene encoding alpha-N-acetylglucosaminidase. Proc. Natl. Acad. Sci. U.S.A. **96**, 14505–14510

10 Yu, W. H., Zhao, K. W., Ryazantsev, S., Rozengurt, N. and Neufeld, E. F. (2000) Short-term enzyme replacement in the murine model of Sanfilippo syndrome type B. Mol. Genet. Metab. **71**, 573–580

11 Fu, H., Samulski, R. J., McCown, T. J., Picornell, Y. J., Fletcher, D. and Muenzer, J. (2002) Neurological correction of lysosomal storage in a mucopolysaccharidosis IIIB mouse model by adeno-associated virus-mediated gene delivery. Mol. Ther. **5**, 42–49

12 Zheng, Y., Ryazantsev, S., Ohmi, K., Zhao, H. Z., Rozengurt, N., Kohn, D. B. and Neufeld, E. F. (2004) Retrovirally transduced bone marrow has a therapeutic effect on brain in the mouse model of mucopolysaccharidosis IIIB. Mol. Genet. Metab. **82**, 286–295

13 Consiglio, A., Quattrini, A., Martino, S., Bensadoun, J. C., Dolcetta, D., Trojani, A., Benaglia, G., Marchesini, S., Cestari, V., Oliverio, A. et al. (2001) In vivo gene therapy of metachromatic leukodystrophy by lentiviral vectors: correction of neuro-pathology and protection against learning impairments in affected mice. Nat. Med. (N.Y.) **7**, 310–316

14 Bosch, A., Perret, E., Desmaris, N., Trono, D. and Heard, J. M. (2000) Reversal of pathology in the entire brain of mucopolysaccharidosis type VII mice after lentivirus-mediated gene transfer. Hum. Gene Ther. **11**, 1139–1150

15 Stein, C. S., Ghodsi, A., Derksen, T. and Davidson, B. L. (1999) Systemic and central nervous system correction of lysosomal storage in mucopolysaccharidosis type VII mice. J. Virol. **73**, 3424–3429

16 Stein, C. S., Kang, Y., Sauter, S. L., Townsend, K., Staber, P., Derksen, T. A., Martins, I., Qian, J., Davidson, B. L. and McCray, P. B. (2001) In vivo treatment of hemophilia A and mucopolysaccharidosis type VII using nonprimate lentiviral vectors. Mol. Ther. **3**, 850–856

17 Villani, G. R. D., Follenzi, A., Vanacore, B., Di Domenico, C., Naldini, L. and Di Natale, P. (2002) Correction of mucopolysaccharidosis type IIIB fibroblasts by lentiviral vector-mediated gene transfer. Biochem. J. **364**, 747–753

18 Di Natale, P., Di Domenico, C., Villani, G. R. D., Lombardo, A., Follenzi, A. and Naldini, L. (2002) In vitro gene therapy of mucopolysaccharidosis type I by lentiviral vectors. Eur. J. Biochem. **269**, 2764–2771

19 Dull, T., Zufferey, R., Kelly, M., Mandel, R. J., Nguyen, M., Trono, D. and Naldini, L. (1998) A third-generation lentivirus vector with a conditional packaging system. J. Virol. **72**, 8463–8471

20 Follenzi, A., Sabatino, G., Lombardo, A., Boccaccio, C. and Naldini, L. (2002) Efficient gene delivery and targeted expression to hepatocytes in vivo by improved lentiviral vectors. Hum. Gene Ther. **13**, 243–260

21 Marsh, J. and Fensom, A. H. (1985) 4-Methylumbelliferyl alpha-N-acetylglucosaminidase activity for diagnosis of Sanfilippo B disease. Clin. Genet. **27**, 258–262

22 Björnsson, S. (1993) Simultaneous preparation and quantitation of proteoglycans by precipitation with alcian blue. Anal. Biochem. **210**, 282–291

23 Bennett, K. L., Hill, R. E., Pietras, D. F., Woodworth-Gutai, M., Kane-Haas, C., Houston, J. M., Heath, J. K. and Hastie, N. D. (1984) Most highly repeated dispersed DNA families in the mouse genome. Mol. Cell. Biol. **4**, 1561–1571

24 Butler, S. L., Hansen, M. S. and Bushman, F. D. (2001) A quantitative assay for HIV DNA integration in vivo. Nat. Med. **7**, 631–634

25 Pfeifer, A., Kessler, T., Yang, M., Baranov, E., Kootstra, N., Cheresh, D. A., Hoffman, R. M. and Verma, I. M. (2001) Transduction of liver cells by lentiviral vectors: analysis in living animals by fluorescence imaging. Mol. Ther. **3**, 319–322

26 Vigna, E. and Naldini, L. (2000) Lentiviral vectors: excellent tools for experimental gene transfer and promising candidates for gene therapy. J. Gene Med. **2**, 308–316

27 Zufferey, R., Dull, T., Mandel, R. J., Bukovsky, A., Quiroz, D., Naldini, L. and Trono, D. (1998) Self-inactivating lentivirus vector for safe and efficient in vivo gene delivery. J. Virol. **72**, 9873–9880

28 Glorioso, J. C., Naldini, L. and Kay, M. A. (2001) Viral vectors for gene therapy: the art of turning infectious agents into vehicles of therapeutics. Nat. Med. **7**, 33–40

29 Pan, D., Gunther, R., Duan, W., Wendell, S., Kaemmerer, W., Kafri, T., Verma, I. M. and Whitley, C. B. (2002) Biodistribution and toxicity studies of VSVG-pseudotyped lentiviral vector after intravenous administration in mice with the observation of in vivo transduction of bone marrow. Mol. Ther. **6**, 19–29

30 Tao, N., Gao, G. P., Parr, M., Johnston, J., Baradet, T., Wilson, J. M., Barsoum, J. and Fawell, S. E. (2000) Sequestration of adenoviral vector by Kupffer cells leads to a nonlinear dose response of transduction in liver. Mol. Ther. **3**, 28–35

31 Brooks, A. I., Stein, C. S., Hughes, S. M., Heth, J., McCray, P. M., Sauter, S. L., Johnston, J. C., Selechta, D. A., Federoff, H. J. and Davidson, B. L. (2002) Functional correction of established central nervous system deficits in an animal model of lysosomal storage disease with feline immunodeficiency virus-based vectors. Proc. Natl. Acad. Sci. U.S.A. **99**, 6216–6221

32 Woloszynek, J. C., Roberts, M., Coleman, T., Vogler, C., Sly, W., Semenkovich, C. F. and Sands, M. S. (2004) Numerous transcriptional alterations in liver persist after short-term enzyme replacement therapy in a murine model of mucopolysaccharidosis type VII. Biochem. J. **379**, 461–469

33 Fu, H., Muenzer, J., Samulski, R. J., Breese, G., Sifford, J., Zeng, X. and McCarty, D. M. (2003) Self-complementary adeno-associated virus serotype 2 vector: global distribution and broad dispersion of AAV-mediated transgene expression in mouse brain. Mol. Ther. **8**, 911–917

34 Jin, H. K. and Schuchman, E. H. (2003) Ex vivo gene therapy using bone marrow-derived cells: combined effects of intracerebral and intravenous transplantation in a mouse model of Niemann-Pick disease. Mol. Ther. **8**, 876–885

35 Vandendriessche, T., Thorrez, L., Naldini, L., Follenzi, A., Moons, L., Berneman, Z., Collen, D. and Chuah, M. K. (2002) Lentiviral vectors containing the human immunodeficiency virus type-1 central polypurine tract can efficiently transduce nondividing hepatocytes and antigen-presenting cells in vivo. Blood **100**, 813–822

36 Follenzi, A., Battaglia, M., Lombardo, L., Annoni, A., Roncarolo, M. G. and Naldini, L. (2004) Targeting lentiviral vector expression to hepatocytes limits transgene-specific immune response and establishes long-term expression of human antihemophilic factor IX in mice. Blood **103**, 3700–3709

Received 7 October 2004/4 January 2005; accepted 13 January 2005
Published as BJ Immediate Publication 13 January 2005, DOI 10.1042/BJ20041702

Available online at www.sciencedirect.com
ScienceDirect
Current Opinion in Structural Biology

Carbohydrate recognition by the mannose-6-phosphate receptors

Jung-Ja P Kim, Linda J Olson and Nancy M Dahms

The two P-type lectins, the 46 kDa cation-dependent mannose-6-phosphate (Man-6-P) receptor (CD-MPR), and the 300 kDa cation-independent Man-6-P receptor (CI-MPR), are the founding members of the growing family of mannose-6-phosphate receptor homology (MRH) proteins. A major cellular function of the MPRs is to transport Man-6-P-containing acid hydrolases from the Golgi to endosomal/lysosomal compartments. Recent advances in the structural analyses of both CD-MPR and CI-MPR have revealed the structural basis for phosphomannosyl recognition by these receptors and provided insights into how the receptors load and unload their cargo. A surprising finding is that the CD-MPR is dynamic, with at least two stable quaternary states, the open (ligand-bound) and closed (ligand-free) conformations, similar to those of hemoglobin. Ligand binding stabilizes the open conformation; changes in the pH of the environment at the cell surface and in endosomal compartments weaken the ligand–receptor interaction and/or weaken the electrostatic interactions at the subunit interface, resulting in the closed conformation.

Addresses
Department of Biochemistry, Medical College of Wisconsin, 8701 Watertown Plank Road, Milwaukee, WI 53226, USA

Corresponding author: Kim, Jung-Ja P (jjkim@mcw.edu), Dahms, Nancy M (ndahms@mcw.edu)

Current Opinion in Structural Biology 2009, **19**:534–542

This review comes from a themed issue on
Carbohydrates and glycoconjugates
Edited by Nathan Sharon, John Gallagher

Available online 2nd October 2009

0959-440X/$ – see front matter

DOI 10.1016/j.sbi.2009.09.002

Introduction

In eukaryotic cells, mannose-6-phosphate receptors (MPRs) mediate the delivery of ~60 different newly synthesized soluble acid hydrolases to the lysosome by binding to mannose-6-phosphate (Man-6-P) residues found on their *N*-linked oligosaccharides. Lysosomal enzymes become differentiated from other proteins in the secretory pathway by acquiring Man-6-P residues in a two-step process: firstly, the GlcNAc-phosphotransferase transfers *N*-acetylglucosamine-1-phosphate to one or two mannose residues on an *N*-glycan to yield a phosphodiester intermediate [1•,2•]. Secondly, α-*N*-acetylglucosaminidase removes the *N*-acetylglucosamine residue in the *trans* Golgi network (TGN) to generate the phosphomonoester, Man-6-P [3] (Figure 1). The resulting MPR/lysosomal enzyme complex is transported from the TGN to the late endosome where the low pH of the compartment induces the complex to dissociate. The released enzymes are packaged into lysosomes [4,5] and the receptors either return to the Golgi to repeat the process or move to the plasma membrane where they function to internalize exogenous ligands (Figure 1). The importance of this phosphomannosyl recognition system in the biogenesis of lysosomes is illustrated by the existence of more than 40 different human lysosomal storage diseases that are estimated to affect 1 in 5000 live births [6]. The discovery of the MPRs originated from studies centered on determining the molecular basis of a lysosomal storage disorder, mucolipidosis II (MLII; also referred to as 'I-cell disease'). The pioneering work of Hickman and Neufeld [7] led to the finding that fibroblasts from MLII patients were capable of internalizing lysosomal enzymes secreted by normal cells, while in contrast, normal fibroblasts were unable to endocytose lysosomal enzymes secreted by MLII fibroblasts. Their hypothesis that lysosomal enzymes contained a recognition tag required for receptor-mediated uptake and transport to lysosomes was later confirmed upon the identification of the tag as Man-6-P [8–10]. I-cell disease is an autosomal recessive disorder caused by a deficiency of GlcNAc-phosphotransferase activity (IUBMB accession number EC 2.7.8.17), which is the enzyme that generates the Man-6-P tag [11] (see Figure 1, step 1).

Two distinct MPRs, the 46 kDa cation-dependent mannose-6-phosphate receptor (CD-MPR) and the ~300 kDa cation-independent mannose-6-phosphate receptor (CI-MPR) are the sole members of the P-type lectin family [12]. The CI-MPR is multifunctional in that it binds proteins bearing the Man-6-P recognition marker as well as the peptide hormone IGF-II (hence it is also called IGF-IIR/CI-MPR) [13–15]. In addition to its intracellular role in lysosome biogenesis and regulation of circulating IGF-II levels, the CI-MPR has been implicated in many other cellular functions because it binds to Man-6-P-containing proteins that are not lysosomal hydrolases. These include transforming growth factor-β (TGF-β) precursor [16], the placental angiogenic hormone proliferin [17], the cytokine leukemia inhibitory factor [18], and the T-cell activation antigen CD26 [19], to name just a few. Functional roles of the cell surface CI-MPR in interactions with these nonlysosomal proteins include activation of TGF-β precursor and renin precursor [20]

Figure 1

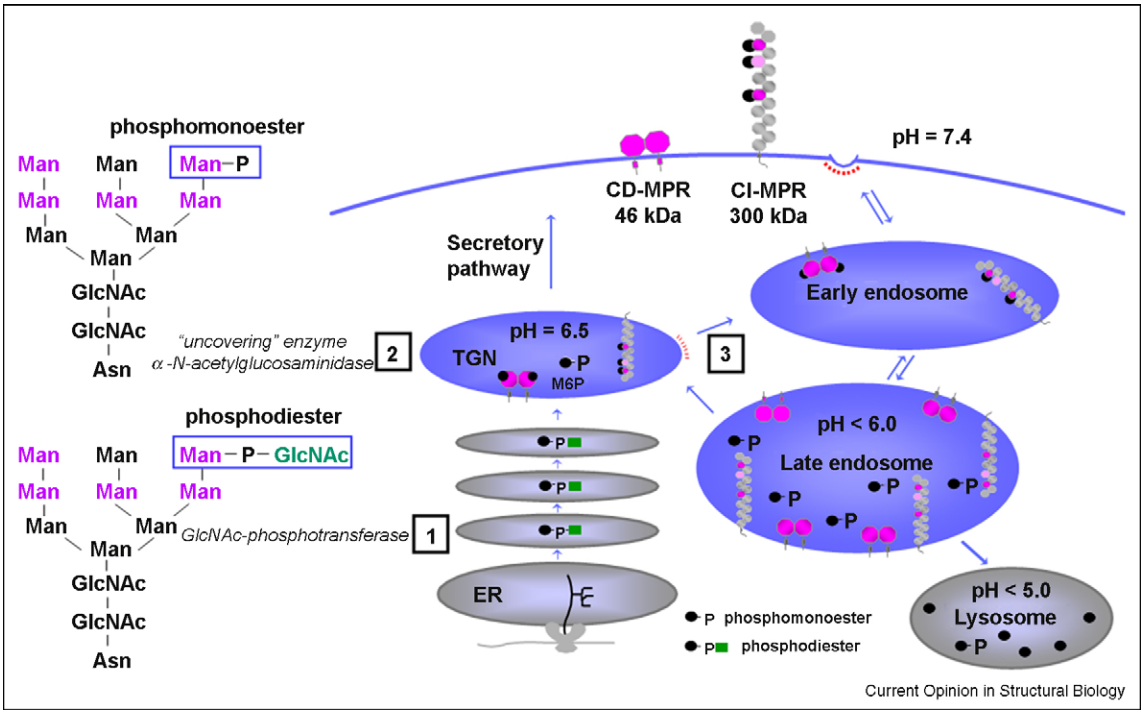

Lysosomal enzyme trafficking. Movements of lysosomal enzymes and MPRs between the various intracellular compartments and the cell surface are shown. Phosphorylation of mannose residues on *N*-linked oligosaccharides occurs in two steps (see text). The five potential sites of phosphorylation are indicated in pink letters. Lysosomal enzymes that acquire the Man-6-P tag in early Golgi compartments bind specifically to MPRs in the Golgi. The resulting receptor–lysosomal enzyme complex is transported from the *trans* Golgi network (TGN) to an early endosomal compartment (step 3) and to an acidified late endosomal compartment where the low pH of the compartment causes dissociation of the complex. Lysosomal enzymes that are not phosphorylated (●), contain a phosphomonoester (●-P), or contain a diester with *N*-acetylglucosamine are shown (●-P-■). The dimeric CD-MPR is depicted as two pink balls and the CI-MPR is shown as 15 repeating balls. The three Man-6-P binding domains of the CI-MPR are depicted as pink balls.

and clearance from the plasma in the case of leukemia inhibitory factor [21]. In addition to IGF-II, the CI-MPR has been shown to interact with a number of proteins that do not have phosphomannosyl residues. These include urokinase-type plasminogen activator receptor (uPAR) [22], plasminogen [23], retinoic acid [24], and heparanase [25•]. Residues essential for uPAR and plasminogen binding have been mapped to domain 1 [26] (Figure 2). However, the nature of their interactions is not clear.

In addition to the two MPRs, several proteins have been identified as containing mannose-6-phosphate receptor homology (MRH) domains [27], including erlectin (a luminal ER protein implicated in the regulation of glycoprotein trafficking) [28], the β-subunit of glucosidase II (also in ER), and GlcNAc-phosphotransferase γ-subunit (in Golgi), all of which are implicated in *N*-glycan recognition [29]. However, studies on their recognition of specific glycans are only beginning to emerge. Recently, human OS-9, which is involved in ER protein quality control, has been shown to interact with mannose-trimmed *N*-glycans [30•]. However, studies will be needed to verify that the MRH domains of these proteins are structurally related to the MPRs.

This review will focus on recent structural studies of the CD-MPR and CI-MPR, with emphasis on how these receptors interact with phosphomannosyl residues. For other aspects of MPRs and related proteins, the reader is referred to articles by Ghosh *et al.* [31•], Gary-Bobo *et al.* [32••], Dahms *et al.* [33••], and Brown *et al.* [34••].

Structures of the CD-MPR and CI-MPR

The MPRs are type 1 transmembrane glycoproteins (Figure 2). The CD-MPR forms a stable homodimer and the CI-MPR exists most likely as a dimer [35]. The bovine CD-MPR is composed of a 28-residue amino-terminal signal sequence, a 159-residue extracytosolic domain, a 25-residue transmembrane region, and a 67-residue carboxyl-terminal cytosolic domain. The six cysteine residues in the extracellular region of the CD-MPR form three disulfide linkages that play an important role in the folding of the molecule. The bovine CI-MPR contains a 44-residue signal sequence, a 2269-residue extracytosolic region, a 23-residue transmembrane region,

Figure 2

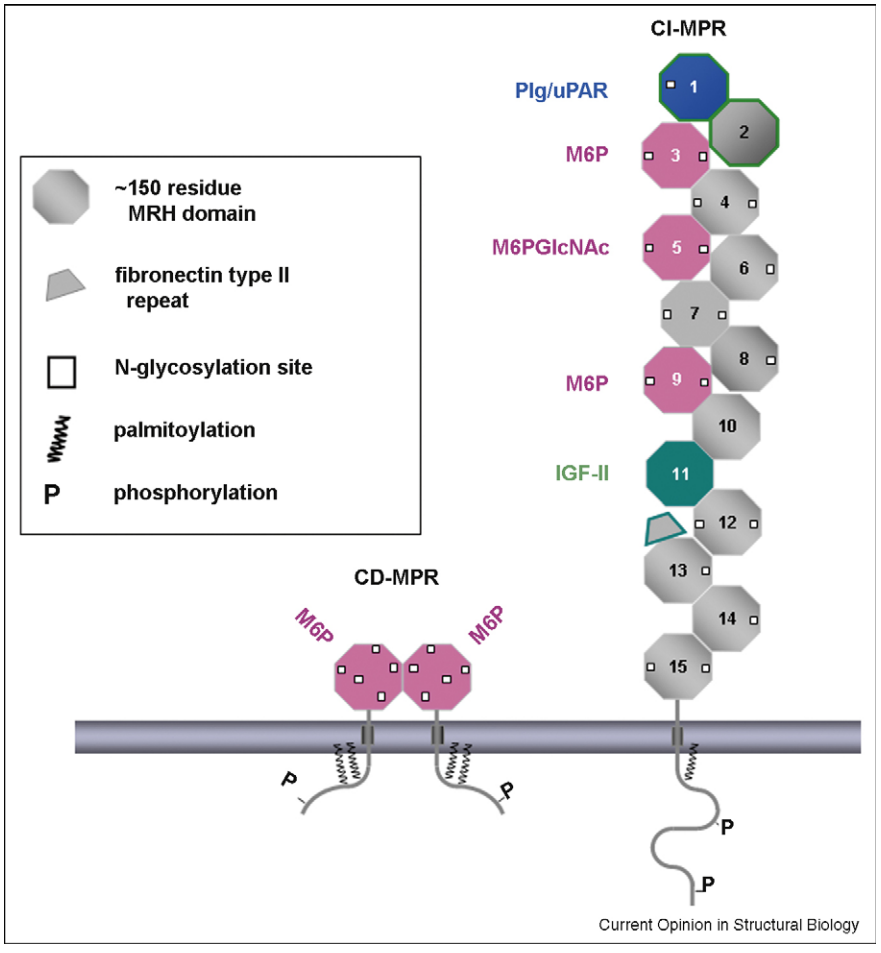

Schematic representation of the CD-MPR (left) and CI-MPR (right). The MPRs are transmembrane glycoproteins. Various post-translational modifications are indicated, including palmitoylation and phosphorylation. The CD-MPR is shown as a dimer with each subunit having one Man-6-P binding site. The 15 repeating domains of the CI-MPR are numbered sequentially from the N-terminus to C-terminus. Domains 3, 5, and 9 bind Man-6-P with domain 5 preferentially binding to phosphodiesters. Domain 1 is known to bind to urokinase plasminogen activator receptor (uPAR) and plasminogen (Plg). Domain 11 binds IGF-II and domain 13 has a fibronectin II insert.

and a 163-residue cytosolic domain. The large extracytosolic region consists of 15 contiguous domains, each of which, when compared to CD-MPR and to each other, has a similar size and significant amino acid sequence identity (14–38%) including cysteine distribution, strongly suggesting that they have similar tertiary structures. Indeed, the crystal structures of the extracytosolic domain of the CD-MPR and domains 1, 2, 3, 11, 12, 13, and 14 of the CI-MPR all have the same fold (Figure 3) [36,37••,38,39] (see below).

The structure of the extracytosolic domain of the CD-MPR in complex with Man-6-P and Mn^{2+} was first determined over 10 years ago [40,41] and has established the overall polypeptide fold of each domain in the P-type lectin family (Figure 3A). The molecule was found to be a dimer, consistent with the predominant oligomeric form of the CD-MPR found in membranes. The overall fold of the CD-MPR monomer is that of a flattened β-barrel consisting of two antiparallel β-sheets, one with four β-strands and the other with five strands, with strand nine interjecting between strands 7 and 8. The dimer interface is formed by two five-stranded β-sheets. The structure of domains 1–3 (the N-terminal 432 residues) of the CI-MPR has been determined in complex with Man-6-P [36,42], confirming that the overall fold of each domain in the CI-MPR is the same as that of the CD-MPR (Figure 3). While the CD-MPR forms a dimer, the N-terminal three domains of the CI-MPR exist as a monomer. The three domains of the CI-MPR form a compact tri-lobed disk and have considerable contact with one another (contact areas between domains range from 8 to 22%). These extensive interactions suggest that the observed three-domain arrangement forms a structural unit within the entire CI-MPR molecule [36], and that the interactions of domain 3 with the loop between

Figure 3

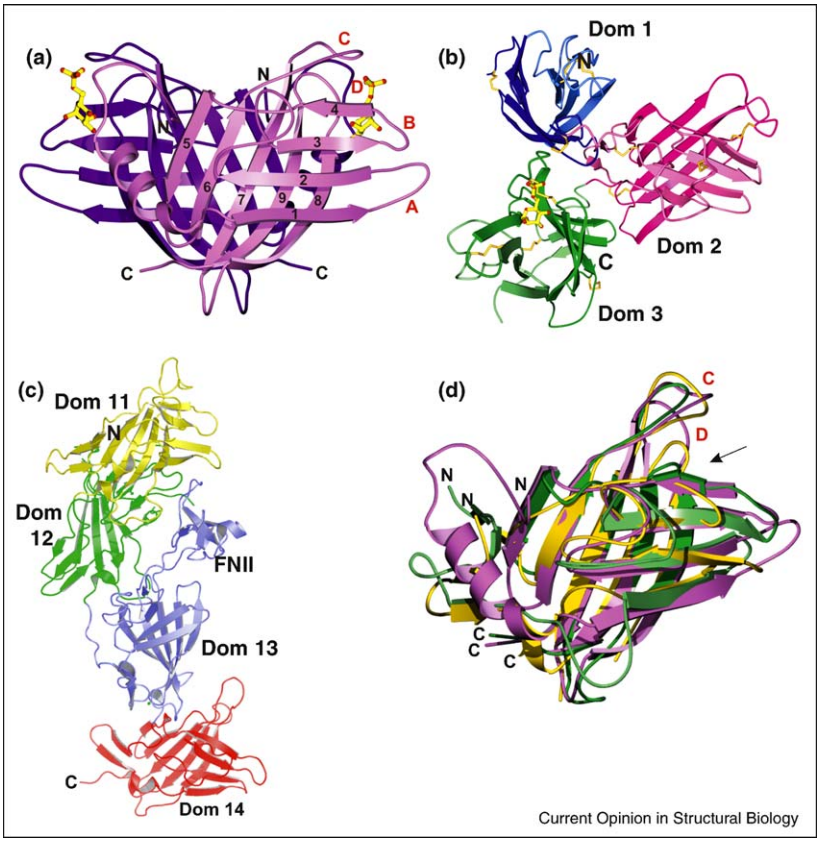

A collage of structures of the CD-MPR and CI-MPR. **(A)** Dimer of the CD-MPR. β-Strands are numbered from N-terminus to C-terminus and loops between strands are labeled in alphabetic order. **(B)** Structure of domains 1–3 of CI-MPR, with bound Man-6-P in domain 3. **(C)** Structure of domains 11–14 of the CI-MPR. N-termini and C-termini are indicated. FNII denotes the fibronectin II insert in domain 13. **(D)** Superposition of the structures of the CD-MPR (monomer, purple) and domains of 3 (green) and 11 (gold) of the CI-MPR, demonstrating that they all have a similar polypeptide fold. For clarity, the structures of domains 1, 2, 12, 13, and 14, whose structures have been determined to have the same fold, are not included in the overlay. The ligand-binding site is indicated with an arrow.

domains 1 and 2 are required for maintaining the architecture of its sugar-binding site.

Comparison of Man-6-P binding pockets in the CD-MPR and CI-MPR

The Man-6-P binding site in the CD-MPR is located at the C-terminal opening of the β-barrel (Figures 3 and 4). One side of the binding pocket is walled off by two loops (loop C, residues G98–R108; and loop D, E134–C141) and the other side is exposed to the solvent, to provide room for the rest of the ligand molecule. The pocket is lined with residues Y45, D103, N104, H105, R135, E133, Y143, Q66, and R111, the latter four of which are found to be essential for Man-6-P binding by mutagenesis studies of CD-MPR [43–45] and domains 3, 5, and 9 of the CI-MPR [46,47•] (Figure 4B). These four signature residues in both the CD-MPR (E133, Y143, Q66, and R111) and domain 3 of CI-MPR (E416, Y421, Q348, and R391) are absolutely conserved (Figure 4C) and interact with the Man-6-P ligand in the same manner, strongly suggesting that the sugar-binding pockets in domains 5 and 9 are also very similar to those of CD-MPR and domain 3 of the CI-MPR (Figure 4A). Indeed, the Man-6-P binding pocket located in domain 3 is essentially the same as that of the CD-MPR, with one exception: the absence of Mn^{2+} which accounts for the metal independence of the CI-MPR. In addition, solution structures of domain 5, which preferentially binds phosphodiesters, with and without a phosphodiester ligand have been determined (L Olson, abstract 216 in Glycobiology 18, 993, 2008). Preliminary results indicate that the overall fold of the isolated domain 5 is similar to that of the other CI-MPR domains and CD-MPR, and mutagenesis studies have demonstrated the essential role of these four signature residues in the lectin activity of domain 5 [47•]. It is interesting to note that the IGF-II binding pocket is located in the homologous position in domain 11 as the Man-6-P binding pocket in domain 3 [37••] (Figure 3D).

Figure 4

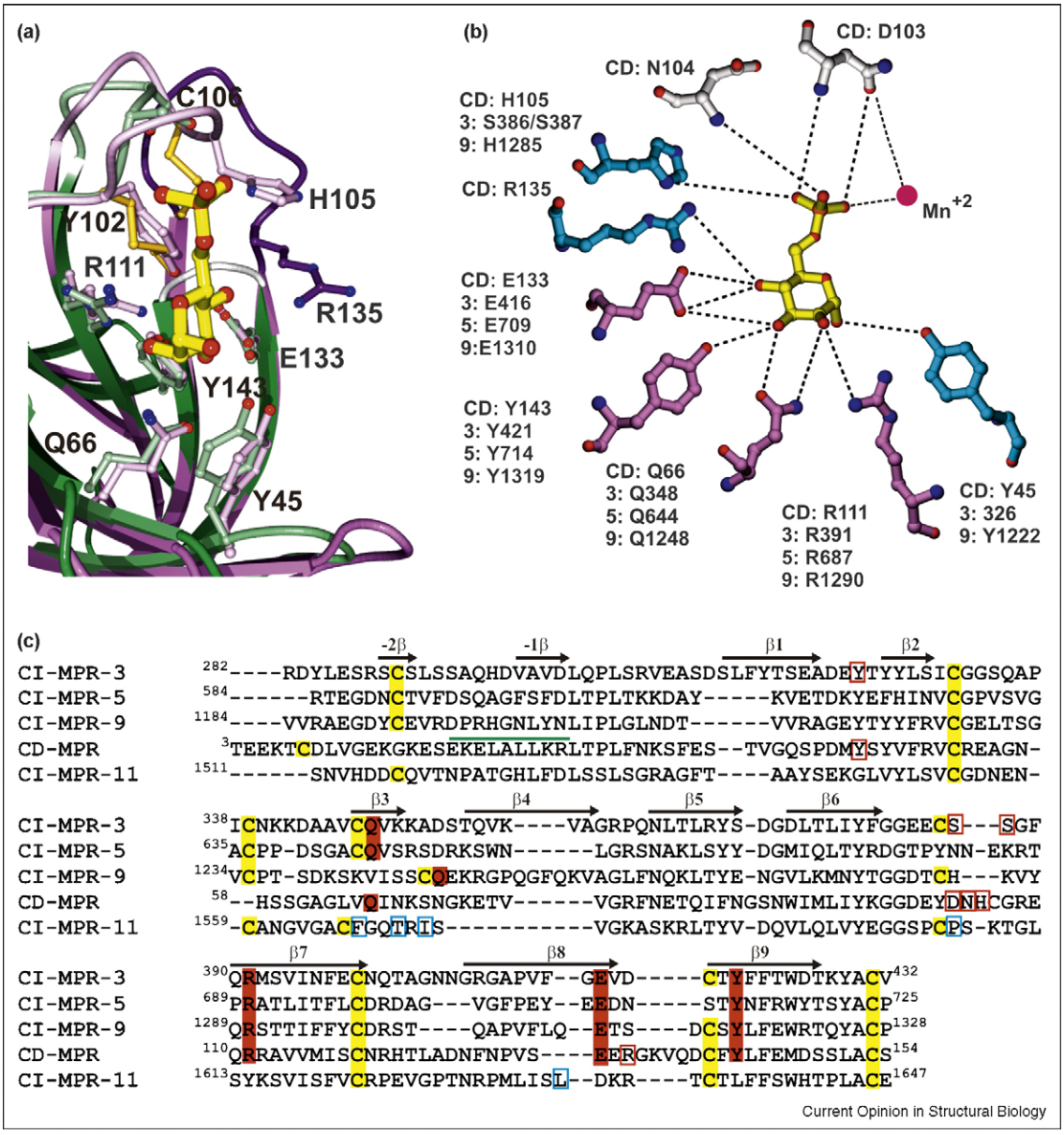

Conservation of the Man-6-P binding site and essential residues for carbohydrate binding. **(A)** Superposition of the Man-6-P binding sites of the CD-MPR (purple) and domain 3 of the CI-MPR (green). The architecture of both binding pockets is essentially the same with the exception of loop D (dark purple, CD-MPR; gray, domain 3), which is shorter in domain 3. **(B)** A schematic drawing showing interactions between Man-6-P and residues in the CD-MPR and their homologous residues in domains 3, 5, and 9 of the CI-MPR. Dotted lines indicate potential hydrogen bonds. Mutational studies have shown that the four residues shown in purple are essential for Man-6-P binding and that mutation of the residues shown in blue partially decreased Man-6-P binding affinity. The two residues in gray have not been tested (N104) or decreased the cation dependency (D103). **(C)** Sequence alignment of domains 3, 5, 9, and 11 of the CI-MPR and the extracytosolic domain of the CD-MPR. The conserved cysteines are highlighted in yellow and the four residues that are essential for Man-6-P binding are highlighted in red. Residues that are within hydrogen bonding distance of Man-6-P in the crystal structures of CD-MPR and domains 1–3 of the CI-MPR, but found to be not essential for Man-6-P binding are boxed in red. Secondary structural elements are indicated with arrows and the single α-helix found in the CD-MPR is indicated with a green cylinder. Residues involved in IGF-II binding in domain 11 of the CI-MPR are boxed in blue.

Inhibition studies using chemically synthesized oligomannosides or neoglycoproteins have shown that the presence of Man-6-P at a terminal position is the major determinant of receptor binding. Furthermore, linear glycans which contain a terminal Man-6-P linked α1,2 to the penultimate mannose were shown to be the most potent inhibitors [48,49]. Recent studies using a novel phosphorylated glycan microarray demonstrate that the CD-MPR demonstrates a preference for glycans containing two phosphomonoesters, whereas the CI-MPR shows

Figure 5

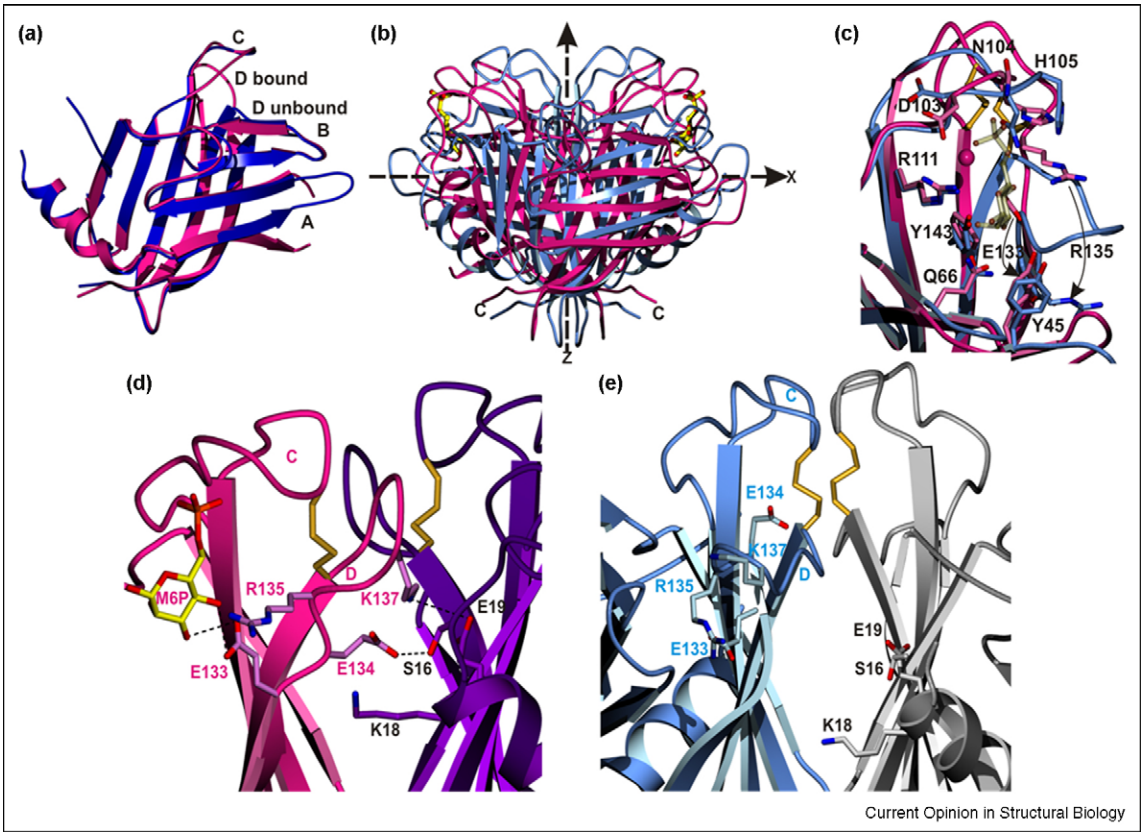

Comparison of the ligand-bound and ligand-free structures of CD-MPR. **(A)** Superposition of the monomer structures bound (pink) and unbound (blue) structures. Note the difference in the conformations of loop D. **(B)** The dimer structures, with the same color scheme as in (A). The molecule is scissoring along its molecular twofold axis (*z*-axis) and twisting along the *x*-axis. The ligand, Man-6-P, is shown with ball-and-sticks. **(C)** Superposition of the ligand-binding sites of the bound (red) and unbound (blue) structures. Loop D in the bound structure forms the side of the binding pocket, while in the unbound structure loop D folds down and occupies the Man-6-P binding site. Mn^{+2} ion in the bound state is denoted as a red ball. The movements of E133 and R135 are indicated (curved arrows). Intersubunit interfaces are shown, including the N-terminus and loop D of the bound (panel **(D)**) and unbound (panel **(E)**) structures. Electrostatic interactions found between the two subunits in the bound structure are disrupted in the unbound structure, resulting in a weaker dimer interface. Disulfide bonds are shown in yellow connecting loops C and D.

little difference in affinity toward glycans containing one or two phosphomonoesters [55].

The CD-MPR is dynamic — comparison of the ligand-bound and ligand-free CD-MPR

The MPRs travel between various cellular compartments during the transportation of their ligand, from TGN (where they bind the ligand) to late endosomes (where they release the ligand). Unlike the CI-MPR, the CD-MPR does not bind ligands at the cell surface. It has been shown that this loading/unloading is facilitated by changes in the pH of each compartment [50]. In order to understand the mechanism of the pH dependence of the ligand binding/release, crystal structures of the CD-MPR have been obtained at various pHs and in the presence and absence of bound Man-6-P [51,52••]. Unexpectedly, regardless of pH, the receptor molecule adopts two conformations: an 'open' conformation found in all structures with bound Man-6-P and a 'closed' conformation observed in all structures without bound ligand (Figure 5). There are three major structural differences between these two states. First, in the open state (i.e. the bound state), the two ligand-binding sites of the dimeric molecule are ~35 Å apart, whereas in the closed (unliganded) state, they are ~26 Å apart. Second, the architecture of the ligand-binding pocket in the closed form differs significantly from the open form (Figure 5C). When the ligand is bound, loop D (residues E134–C141) forms one wall of the binding pocket. When the ligand is absent, loop D folds into the binding pocket, occupying the same space where the sugar molecule binds and thereby keeps the position of the sugar-binding residues unchanged. Lastly, this loop D movement disrupts electrostatic interactions between the two subunits, releasing intersubunit salt bridges, causing the two subunits to slide and twist at their interface which results in the 'closed' form (Figure 5B and C). Thus, the movements involved in the bound-to-unbound transition of the

CD-MPR are reminiscent of those in the oxy-to-deoxy transition of hemoglobin. However, whether the CD-MPR has ligand-binding cooperativity has not been studied. The overall movement of the bound-to-unbound transition can be described as a 'scissoring and twisting' motion between the two subunits at the dimer interface. The implication of the existence of these two states is that the CD-MPR must be able to readily transition between these two conformations as it travels to the different cellular compartments, with the unique environment of each compartment (e.g. Golgi, cell surface, endosome) impacting the equilibrium between the two states.

Mechanisms of ligand binding and release by the CD-MPR

From the above structural studies, plausible mechanisms for the dissociation of lysosomal enzymes in the acidic endosome (pH <6.0) and at the cell surface (pH 7.4) have been proposed [52••]. The structure of the bound form of CD-MPR has three intersubunit ion pairs that 'tie' loop D of one subunit to the other subunit (K18 and E19 of one subunit to E134 and K138 of the other subunit, respectively) (Figure 5D). In the acidic environment of the endosome, the disruption of intersubunit electrostatic interactions may trigger the ligand release by protonation of the carboxyl groups of the glutamates and aspartate (Figure 5D and E). In addition, E133, one of the essential residues for binding of Man-6-P, might also be protonated in the endosome and weaken its binding to Man-6-P, promoting release of the bound ligand (Figure 5D). On the other hand, at the cell surface, deprotonation of H105 and the phosphate moiety of Man-6-P (both of which interact with each other in the bound conformation) are most likely responsible for the release of the ligand (Figures 4 and 5C). To probe directly the role of the electrostatic interactions between the two subunits, specifically the salt bridge between E19 and K137, a double mutant (E19Q/K137M) has been analyzed by surface plasmon resonance. The mutant CD-MPR lacking the intersubunit salt bridge binds lysosomal enzymes with ~100-fold lower affinity, clearly demonstrating the critical role of the ionic interactions between the two subunits in stabilizing the bound conformer of the CD-MPR.

Conclusions

Although we have accumulated considerable knowledge on the MPRs regarding the structural basis for their phosphomannosyl recognition and the mechanisms of the cargo loading and unloading for the CD-MPR, there still remain many outstanding questions. It is interesting to note that all ligand-binding sites of CI-MPR are located at odd-numbered domains, that is, domains 3, 5, and 9 for Man-6-P binding and domain 11 for IGF-II, as well as domain 1 which is found to interact with plasminogen and uPAR. What are the roles of the remaining domains? Do even-numbered domains function only as spacers and/or support for the functional domains? What are the mechanisms of ligand binding and release for the CI-MPR, which must be very different from those of CD-MPR? Answers to these questions must await further biochemical and structural studies of the CI-MPR including fragments containing overlapping ranges of domains. It is also intriguing that the CI-MPR complements the two enzymes that make the phosphomannosyl tag by being able to bind to the products of both the first and the second enzymes of the two-step process. Is this purely for redundancy? Furthermore, the mechanisms that govern the MPRs' trafficking to different subcellular compartments are not clearly known. MPRs are present in TGN, endosomes, and plasma membrane, but absent in lysosomes. They cycle constitutively between these compartments and this trafficking is directed by sorting signals that reside in the cytosolic tails of the receptors. Currently, only the structures of peptides (12 or 13 residues) that contain the di-leucine motif in the cytosolic tails of CD-MPR and CI-MPR, in complex with the VHS domain of human GGA (Golgi-localized, γ-ear-containing, ADP-ribosylating-factor-binding) proteins are known [53,54]. Thus, in order to gain a clearer picture of the factors that regulate the interaction of the MPRs' cytoplasmic region with numerous cytosolic adaptor proteins, further structural analyses are needed.

Acknowledgement

This work was supported by NIH grant DK42667 to NMD and J-JPK.

References and recommended reading

Papers of particular interest, published within the period of review, have been highlighted as:

- • of special interest
- •• of outstanding interest

1. • Gelfman CM, Vogel P, Issa TM, Turner CA, Lee WS, Kornfeld S, Rice DS: **Mice lacking alpha/beta subunits of GlcNAc-1-phosphotransferase exhibit growth retardation, retinal degeneration, and secretory cell lesions**. *Invest Ophthalmol Vis Sci* 2007, **48**:5221-5228.

GlcNAc-1 phosphotransferase catalyzes the first step of the two-step process in the acquisition of mannose-6-phosphate on *N*-linked oligosaccharides of lysosomal enzymes. Mice deficient in the phosphotransferase gene exhibit severe retinal degeneration in addition to the features observed in patients with mucolipidosis II. Authors suggest a connection between retinal diseases and lysosomal storage disorders via GlcNAc-phosphotransferase.

2. • Lee WS, Payne BJ, Gelfman CM, Vogel P, Kornfeld S: **Murine UDP-GlcNAc:lysosomal enzyme *N*-acetylglucosamine-1-phosphotransferase lacking the gamma-subunit retains substantial activity toward acid hydrolases**. *J Biol Chem* 2007, **282**:27198-27203.

Along with Ref. [1•], this article characterizes the phosphotransferase. The paper shows that the α/β subunits of the enzyme, in addition to their catalytic function, have some ability to recognize acid hydrolases as specific substrates.

3. Varki A, Sherman W, Kornfeld S: **Demonstration of the enzymatic mechanisms of alpha-*N*-acetyl-D-glucosamine-1-phosphodiester *N*-acetylglucosaminidase (formerly called alpha-*N*-acetylglucosaminylphosphodiesterase) and lysosomal alpha-*N*-acetylglucosaminidase**. *Arch Biochem Biophys* 1983, **222**:145-149.

4. Le Borgne R, Hoflack B: **Protein transport from the secretory to the endocytic pathway in mammalian cells**. *Biochim Biophys Acta* 1998, **1404**:195-209.

5. Mullins C, Bonifacino JS: **The molecular machinery for lysosome biogenesis**. *Bioessays* 2001, **23**:333-343.

6. Meikle PJ, Hopwood JJ: **Lysosomal storage disorders: emerging therapeutic options require early diagnosis**. *Eur J Pediatr* 2003, **162**:S34-S37.

7. Hickman S, Neufeld EF: **A hypothesis for I-cell disease: defective hydrolases that do not enter lysosomes**. *Biochem Biophys Res Commun* 1972, **49**:992-999.

8. Kaplan A, Fischer D, Achord D, Sly W: **Phosphohexosyl recognition is a general characteristic of pinocytosis of lysosomal glycosidases by human fibroblasts**. *J Clin Invest* 1977, **60**:1088-1093.

9. Distler J, Hieber V, Sahagian G, Schmickel R, Jourdian GW: **Identification of mannose 6-phosphate in glycoproteins that inhibit the assimilation of beta-galactosidase by fibroblasts**. *Proc Natl Acad Sci U S A* 1979, **76**:4235-4239.

10. Natowicz MR, Chi MM, Lowry OH, Sly WS: **Enzymatic identification of mannose 6-phosphate on the recognition marker for receptor-mediated pinocytosis of beta-glucuronidase by human fibroblasts**. *Proc Natl Acad Sci U S A* 1979, **76**:4322-4326.

11. Reitman ML, Kornfeld S: **Lysosomal enzyme targeting. *N*-Acetylglucosaminylphosphotransferase selectively phosphorylates native lysosomal enzymes**. *J Biol Chem* 1981, **256**:11977-11980.

12. Drickamer K, Taylor ME: **Biology of animal lectins**. *Annu Rev Cell Biol* 1993, **9**:237-264.

13. MacDonald RG, Pfeffer SR, Coussens L, Tepper MA, Brocklebank CM, Mole JE, Anderson JK, Chen E, Czech MP, Ullrich A: **A single receptor binds both insulin-like growth factor II and mannose-6-phosphate**. *Science* 1988, **239**:1134-1137.

14. Schmidt B, Kiecke-Siemsen C, Waheed A, Braulke T, von Figura K: **Localization of the insulin-like growth factor II binding site to amino acids 1508–1566 in repeat 11 of the mannose 6-phosphate/insulin-like growth factor II receptor**. *J Biol Chem* 1995, **270**:14975-14982.

15. Dahms NM, Wick DA, Brzycki-Wessell MA: **The bovine mannose 6-phosphate/insulin-like growth factor II receptor. Localization of the insulin-like growth factor II binding site to domains 5–11**. *J Biol Chem* 1994, **269**:3802-3809.

16. Purchio AF, Cooper JA, Brunner AM, Lioubin MN, Gentry LE, Kovacina KS, Roth RA, Marquardt H: **Identification of mannose 6-phosphate in two asparagine-linked sugar chains of recombinant transforming growth factor-beta 1 precursor**. *J Biol Chem* 1988, **263**:14211-14215.

17. Lee SJ, Nathans D: **Proliferin secreted by cultured cells binds to mannose 6-phosphate receptors**. *J Biol Chem* 1988, **263**:3521-3527.

18. Blanchard F, Raher S, Duplomb L, Vusio P, Pitard V, Taupin JL, Moreau JF, Hoflack B, Minvielle S, Jacques Y *et al.*: **The mannose 6-phosphate/insulin-like growth factor II receptor is a nanomolar affinity receptor for glycosylated human leukemia inhibitory factor**. *J Biol Chem* 1998, **273**:20886-20893.

19. Ikushima H, Munakata Y, Ishii T, Iwata S, Terashima M, Tanaka H, Schlossman SF, Morimoto C: **Internalization of CD26 by mannose 6-phosphate/insulin-like growth factor II receptor contributes to T cell activation**. *Proc Natl Acad Sci U S A* 2000, **97**:8439-8444.

20. van Kesteren CA, Danser AH, Derkx FH, Dekkers DH, Lamers JM, Saxena PR, Schalekamp MA: **Mannose 6-phosphate receptor-mediated internalization and activation of prorenin by cardiac cells**. *Hypertension* 1997, **30**:1389-1396.

21. Blanchard F, Duplomb L, Raher S, Vusio P, Hoflack B, Jacques Y, Godard A: **Mannose 6-phosphate/insulin-like growth factor II receptor mediates internalization and degradation of leukemia inhibitory factor but not signal transduction**. *J Biol Chem* 1999, **274**:24685-24693.

22. Nykjaer A, Christensen EI, Vorum H, Hager H, Petersen CM, Roigaard H, Min HY, Vilhardt F, Moller LB, Kornfeld S *et al.*: **Mannose 6-phosphate/insulin-like growth factor-II receptor targets the urokinase receptor to lysosomes via a novel binding interaction**. *J Cell Biol* 1998, **141**:815-828.

23. Godar S, Horejsi V, Weidle UH, Binder BR, Hansmann C, Stockinger H: **M6P/IGFII-receptor complexes urokinase receptor and plasminogen for activation of transforming growth factor-beta1**. *Eur J Immunol* 1999, **29**:1004-1013.

24. Kang JX, Li Y, Leaf A: **Mannose-6-phosphate/insulin-like growth factor-II receptor is a receptor for retinoic acid**. *Proc Natl Acad Sci U S A* 1997, **94**:13671-13676.

25. • Wood RJ, Hulett MD: **Cell surface-expressed cation-independent mannose 6-phosphate receptor (CD222) binds enzymatically active heparanase independently of mannose 6-phosphate to promote extracellular matrix degradation**. *J Biol Chem* 2008, **283**:4165-4176.
Purified platelet heparanase was shown to bind the human CI-MPR expressed on the surface of a transfected mouse L cell line, demonstrating that the CI-MPR is a cell surface receptor for heparanase and its binding to the receptor is independent of mannose-6-phospate binding.

26. Leksa V, Godar S, Cebecauer M, Hilgert I, Breuss J, Weidle UH, Horejsi V, Binder BR, Stockinger H: **The N terminus of mannose 6-phosphate/insulin-like growth factor 2 receptor in regulation of fibrinolysis and cell migration**. *J Biol Chem* 2002, **277**:40575-40582.

27. Dodd RB, Drickamer K: **Lectin-like proteins in model organisms: implications for evolution of carbohydrate-binding activity**. *Glycobiology* 2001, **11**:71R-79R.

28. Cruciat CM, Hassler C, Niehrs C: **The MRH protein erlectin is a member of the endoplasmic reticulum synexpression group and functions in *N*-glycan recognition**. *J Biol Chem* 2006, **281**:12986-12993.

29. Munro S: **The MRH domain suggests a shared ancestry for the mannose 6-phosphate receptors and other *N*-glycan-recognising proteins**. *Curr Biol* 2001, **11**:R499-501.

30. • Hosokawa N, Kamiya Y, Kamiya D, Kato K, Nagata K: **Human OS-9, a lectin required for glycoprotein ERAD, recognizes mannose-trimmed *N*-glycans**. *J Biol Chem* 2009, **284**:17061-17068.
A new member of the MRH family, human OS-9, has been studied for its carbohydrate specificity and the results suggest that human OS-9 specifically binds *N*-glycans that lack the terminal mannose from the C-branch.

31. • Ghosh P, Dahms NM, Kornfeld S: **Mannose 6-phosphate receptors: new twists in the tale**. *Nat Rev Mol Cell Biol* 2003, **4**:202-213.
An older but still excellent review on the transport of acid hydrolases from the *trans* Golgi network to lysosomes in mammalian cells.

32. •• Gary-Bobo M, Nirde P, Jeanjean A, Morere A, Garcia M: **Mannose 6-phosphate receptor targeting and its applications in human diseases**. *Curr Med Chem* 2007, **14**:2945-2953.
This review focuses on the cation-independent mannose-6-phosphate receptor, highlighting the synthesis and potential use of high-affinity mannose-6-phosphate analogs that can target this receptor. These analogs could be used for the delivery of specific compounds to lysosomes to be used in enzyme replacement therapies of lysosomal diseases.

33. •• Dahms NM, Olson LJ, Kim JJ: **Strategies for carbohydrate recognition by the mannose 6-phosphate receptors**. *Glycobiology* 2008, **18**:664-678.
This is a comprehensive review of the two mannose-6-phosphate receptors regarding their functions, structures, and their ligand specificities. The review also discusses evolutionary aspect of the receptors and other members of the MRH family.

34. •• Brown J, Jones EY, Forbes BE: **Interactions of IGF-II with the IGF2R/cation-independent mannose-6-phosphate receptor mechanism and biological outcomes**. *Vitam Horm* 2009, **80**:699-719.
A review focused on molecular interactions between the IGF-IIR/CI-MPR and IGF-II and other ligands, highlighting the recent structural analyses of domains 11–14 with and without bound IGF-II. Also detailed discussion of the underlying mechanism of action of the IGF-IIR/CI-MPR is presented.

35. Hartman MA, Kreiling JL, Byrd JC, MacDonald RG: **High-affinity ligand binding by wild-type/mutant heteromeric complexes of the mannose 6-phosphate/insulin-like growth factor II receptor**. *FEBS J* 2009, **276**:1915-1929.

36. Olson LJ, Yammani RD, Dahms NM, Kim JJ: **Structure of uPAR, plasminogen, and sugar-binding sites of the 300 kDa mannose 6-phosphate receptor**. *EMBO J* 2004, **23**:2019-2028.

37. •• Brown J, Delaine C, Zaccheo OJ, Siebold C, Gilbert RJ, van Boxel G, Denley A, Wallace JC, Hassan AB, Forbes BE *et al.*: **Structure and functional analysis of the IGF-II/IGF2R interaction**. *EMBO J* 2008, **27**:265-276.
Crystal structures of IGF-IIR/cation-independent mannose-6-phosphate receptor domains 11–12, 12–13–14, and domains 11–12–13/IGF-II complex are described. The structures reveal that each domain has the same polypeptide fold as that of domains 1–2–3 and extracytosolic domain of the cation-dependent receptor. The complex structure combined with mutagenesis analyses reveals the IGF-II binding hotspot on the receptor.

38. Uson I, Schmidt B, von Bulow R, Grimme S, von Figura K, Dauter M, Rajashankar KR, Dauter Z, Sheldrick GM: **Locating the anomalous scatterer substructures in halide and sulfur phasing**. *Acta Crystallogr Sect D-Biol Crystallogr* 2003, **59**:57-66.

39. Brown J, Esnouf RM, Jones MA, Linnell J, Harlos K, Hassan AB, Jones EY: **Structure of a functional IGF2R fragment determined from the anomalous scattering of sulphur**. *EMBO J* 2002, **21**:1054-1062.

40. Roberts DL, Weix DJ, Dahms NM, Kim J-JP: **Molecular basis of lysosomal enzyme recognition: three-dimensional structure of the cation-dependent mannose 6-phosphate receptor**. *Cell* 1998, **93**:639-648.

41. Olson LJ, Zhang J, Lee YC, Dahms NM, Kim J-JP: **Structural basis for recognition of phosphorylated high mannose oligosaccharides by the cation-dependent mannose 6-phosphate receptor**. *J Biol Chem* 1999, **274**:29889-29896.

42. Olson LJ, Dahms NM, Kim JJ: **The N-terminal carbohydrate recognition site of the cation-independent mannose 6-phosphate receptor**. *J Biol Chem* 2004, **279**:34000-34009.

43. Wendland M, Waheed A, von Figura K, Pohlmann R: **Mr 46,000 mannose 6-phosphate receptor. The role of histidine and arginine residues for binding of ligand**. *J Biol Chem* 1991, **266**:2917-2923.

44. Olson LJ, Hancock MK, Dix D, Kim J-JP, Dahms NM: **Mutational analysis of the binding site residues of the bovine cation-dependent mannose 6-phosphate receptor**. *J Biol Chem* 1999, **274**:36905-36911.

45. Sun G, Zhao H, Kalyanaraman B, Dahms NM: **Identification of residues essential for carbohydrate recognition and cation dependence of the 46-kDa mannose 6-phosphate receptor**. *Glycobiology* 2005, **15**:1136-1149.

46. Hancock MK, Haskins DJ, Sun G, Dahms NM: **Identification of residues essential for carbohydrate recognition by the insulin-like growth factor II/mannose 6-phosphate receptor**. *J Biol Chem* 2002, **277**:11255-11264.

47. • Chavez CA, Bohnsack RN, Kudo M, Gotschall RR, Canfield WM, Dahms NM: **Domain 5 of the cation-independent mannose 6-phosphate receptor preferentially binds phosphodiesters (mannose 6-phosphate *N*-acetylglucosamine ester)**. *Biochemistry* 2007, **46**:12604-12617.
Mutations of domain 5 of the cation-independent mannose-6-phosphate receptor were studied by surface plasmon resonance analyses, demonstrating that domain 5 is unique among lectins because of its ability to bind phosphodiesters.

48. Distler JJ, Guo JF, Jourdian GW, Srivastava OP, Hindsgaul O: **The binding specificity of high and low molecular weight phosphomannosyl receptors from bovine testes. Inhibition studies with chemically synthesized 6-*O*-phosphorylated oligomannosides**. *J Biol Chem* 1991, **266**:21687-21692.

49. Tomoda H, Ohsumi Y, Ichikawa Y, Srivastava OP, Kishimoto Y, Lee YC: **Binding specificity of D-mannose 6-phosphate receptor of rabbit alveolar macrophages**. *Carbohydr Res* 1991, **213**:37-46.

50. Imort M, Zuhlsdorf M, Feige U, Hasilik A, von Figura K: **Biosynthesis and transport of lysosomal enzymes in human monocytes and macrophages. Effects of ammonium chloride, zymosan and tunicamycin**. *Biochem J* 1983, **214**:671-678.

51. Olson LJ, Zhang J, Dahms NM, Kim J-JP: **Twists and turns of the CD-MPR: ligand-bound versus ligand-free receptor**. *J Biol Chem* 2002, **277**:10156-10161.

52. •• Olson LJ, Hindsgaul O, Dahms NM, Kim JJ: **Structural insights into the mechanism of pH-dependent ligand binding and release by the cation-dependent mannose 6-phosphate receptor**. *J Biol Chem* 2008, **283**:10124-10134.
Crystal structures of the cation-dependent mannose-6-phosphate receptor at various pHs and with and without mannose-6-phosphate (ligand) were determined, demonstrating that the molecule is dynamic and is able to transition between two stable conformations. The paper presents detailed description of the mechanisms of ligand binding and release by the receptor.

53. Misra S, Puertollano R, Kato Y, Bonifacino JS, Hurley JH: **Structural basis for acidic-cluster-dileucine sorting-signal recognition by VHS domains**. *Nature* 2002, **415**:933-937.

54. Shiba T, Takatsu H, Nogi T, Matsugaki N, Kawasaki M, Igarashi N, Suzuki M, Kato R, Earnest T, Nakayama K *et al.*: **Structural basis for recognition of acidic-cluster dileucine sequence by GGA1**. *Nature* 2002, **415**:937-941.

55. Song X, Lasanajak Y, Olson LJ, Boonen M, Dahms NM, Kornfeld S, Cummings RD, Smith DF: **Glycan Microarray Analysis of P-Type Lectins Reveals Distinct Phospho-Mannose Glycan Recognition**. *J. Biol. Chem.* 2009, in press.